Differential Modulations for Multinode Cooperative Communications

Thanongsak Himsoon, *Member, IEEE*, W. Pam Siriwongpairat, *Member, IEEE*, Weifeng Su, *Member, IEEE*, and K. J. Ray Liu, *Fellow, IEEE*

***Abstract*—This paper proposes and analyzes differential modulation schemes for two cooperation protocols in multinode cooperative wireless networks; namely, multinode differential amplify-and-forward scheme (DiffAF) and multinode differential decode-and-forward scheme (DiffDF). In the DiffAF scheme, with knowledge of long-term average of received signals from all communication links, the destination efficiently combines signals from direct and all multiple-relay links to improve communication reliability. In the DiffDF scheme, by utilizing a decision threshold at each relay-destination link, the destination efficiently combines signals from the direct link and each relay link whose signal amplitude is larger than the threshold. For the DiffAF scheme, an exact bit error rate (BER) formulation based on optimum combining is provided for differential M-ary phase shift keying (DMPSK) modulation, and it serves as a performance benchmark of the proposed DiffAF scheme. In addition, BER upper bounds, BER lower bounds, and simple BER approximations are derived. Then, optimum power allocation is provided to further improve performance of the DiffAF scheme. Based on the tight BER approximation, the optimum power allocation can be simply obtained through a single dimensional search. In case of the DiffDF scheme, the performance of DMPSK modulation is analyzed. First, a BER formulation for DMPSK modulation is derived. Next, an approximate BER formulation of the DiffDF scheme is obtained, and a tractable BER lower bound is derived to provide further insights. Then, the performance of the DiffDF scheme is enhanced by jointly optimizing power allocation and decision thresholds with an aim to minimize the BER. Finally, simulation results under the two proposed cooperation protocols are given to validate their merit and support the theoretical analysis.**

***Index Terms*—Bit error rate (BER), cooperative communications, differential modulation, multinode wireless networks, virtual multiple-input–multiple-output (MIMO).**

I. Introduction

RECENTLY, cooperative communications have gained much attention due to the ability to explore inherent spatial diversity available in relay channels by forming a virtual antenna array among cooperating nodes. In this strategy, when a node has information to transmit, it cooperates with other nodes which helps forward the information to an intended destination. To explore such inherent spatial diversity, various cooperation protocols have been proposed based on relay processing, e.g., decode-and-forward (DF) and amplify-and-forward (AF) [1]. Under the DF protocol, each relay decodes the received signal from the source, and then forwards the decoded information to the destination. Under the AF protocol, on the other hand, each relay amplifies the received signal and then forwards the amplified signal to the destination. In [2] and [3], a concept of user cooperation has been introduced for a two-user code division multiple access (CDMA) cooperation system by which orthogonal codes are used among active users to avoid multiple access interference. The work in [4] focuses on rigorous analysis of exact symbol error rate (SER) and optimum power allocation for the DF protocol for two-user cooperation systems. The work in [5] proposed a class of coherent multinode DF cooperation protocols with arbitrary N-relay nodes in which each relays combines signal from the source and the previous $m\,(1 \leq m \leq N-1)$ relays. In [6]–[8], an idea of distributed space-time coding has been considered by which all cooperation nodes form virtual antenna array and synchronously encode information using existing space-time codes.

However, most of the works in [1]–[8] assume that the destination has perfect knowledge of channel state information (CSI) of all transmission links. While in some scenarios, e.g., slow fading environment, the CSI is likely to be acquired by the use of pilot symbols, it may not be possible in fast fading environment. In addition, it is questionable on how the destination can obtain source-relay channel perfectly through pilot signal forwarding without noise amplification. Moreover, the computational overhead for channel estimation increases in proportion to the product of number of transmit antennas at the source node and number of relaying nodes.

Differential modulation has been well accepted as a modulation technique that provides a good tradeoff between receiver complexity and performance. In differential phase-shift keying (DPSK) [9], efficient decoding relies on constant phase responses of the channel from one time sample to the next. Therefore, perfect CSI is not required at the differential decoder. The merit of bypassing channel estimation makes differential modulation a viable candidate to be deployed in cooperative communication so as to reduce receiver complexity and signal overheads. In [10], error performance of coherent/differential modulations for a specific two-hop relay system have been investigated. In [11], a framework of noncoherent communication employing frequency shift keying modulation has been proposed for DF cooperation systems. However, the framework

Manuscript received December 14, 2006; revised October 28, 2007. The associate editor coordinating the review of this manuscript and approving it for publication was Dr. Mounir Ghogho.

T. Himsoon and W. P. Siriwongpairat are with the Meteor Communications Corporation, Kent, WA 98032 USA (e-mail: KHimsoon@meteorcomm.com; PSiriwongpairat@meteorcomm.com).

W. Su is with the Department of Electrical Engineering, State University of New York (SUNY) at Buffalo, Buffalo, NY 14260 USA (e-mail: weifeng@eng.buffalo.edu).

K. J. R. Liu is with the Department of Electrical and Computer Engineering and Institute for Systems Research, University of Maryland, College Park, MD 20742 USA (e-mail: kjrliu@umd.edu).

Digital Object Identifier 10.1109/TSP.2008.917358

does not fit to a general M-ary differential phase-shift keying (MDPSK) and the AF cooperation system.

The related works on differential cooperative schemes have been considered in [12]–[15]. In [12], a differential scheme for the DF protocol has been investigated for a two-user cooperation system in which the two users transmit signal in an Alamouti-like fashion. In [13] and [14], a differential scheme for the AF protocol and its error rate performance has been investigated for two-user cooperation systems. In addition, [14] provided a simple bit error rate (BER) performance formulation of the proposed scheme, which is derived based on the moment generating function method, and this formulation is used for optimally allocating power among nodes to further improve the system performance. However, the simple BER formulation is complicated and optimum power allocation scheme is obtained only through exhaustive numerical search. In [15], a threshold-based differential cooperative scheme employing the DF protocol has been proposed for a two-user wireless network. A tight BER approximation is provided, and optimum power allocation and threshold are numerically determined to further enhance performance. In [16], a two-node differential DF scheme is proposed where power allocation at the relay is proportioned to the channel variances at the source-relay link and the relay-destination link. The power allocation scheme in [16] relies on assumptions that channels are quasi-static over a frame period, and the relay receives reliable feedback of channel variance of the relay-destination link. The work in [15], on the other hand, is applicable to more relaxed channel, which can vary symbol by symbol, and requires no channel feedback. Nevertheless, most of the existing differential cooperative schemes focus on two-node wireless networks.

This paper proposes differential modulation schemes for AF and DF cooperative communications in multinode cooperative networks. Due to their low-complexity implementations, the proposed schemes can be deployed in sensor and ad hoc networks in which multinode signal transmissions are necessary for reliable communications among nodes. In this work, the destination in the DiffAF scheme requires only long-term average of the received signals to efficiently combine signals from all communications links. In the DiffDF scheme, each relay decodes the received signal and it forwards only correctly decoded symbols to the destination. A number of decision thresholds that correspond to the number of relays are used at the destination to efficiently combine received signals from each relay-destination link with that from the direct link. BER performance of both DiffAF and DiffDF schemes is analyzed and optimum power allocation is provided to further improve the system performance. In case of the DiffAF scheme, we provide an exact BER formulation based on optimum combining weights for MDPSK modulation. The obtained BER formulation serves as a performance benchmark of the DiffAF scheme. In addition, BER upper bounds and simple BER approximations are provided. One of the tight BER approximations allows us to optimize the power allocation through a simple single-dimensional search. In case of the DiffDF scheme, a BER formulation with DMPSK modulation is derived. In addition, BER approximation and a tractable BER lower bound are provided. Then, power allocation and thresholds are jointly optimized. Simulation results are shown to validate the merit of the proposed DiffAF/DiffDF schemes and support the theoretical analysis.

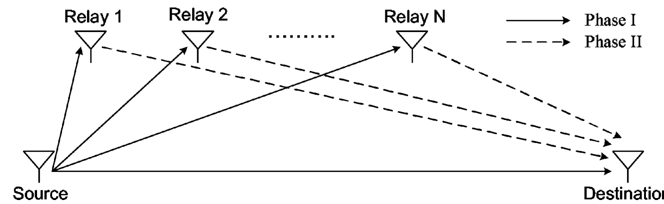

Fig. 1. Multinode differential AF scheme.

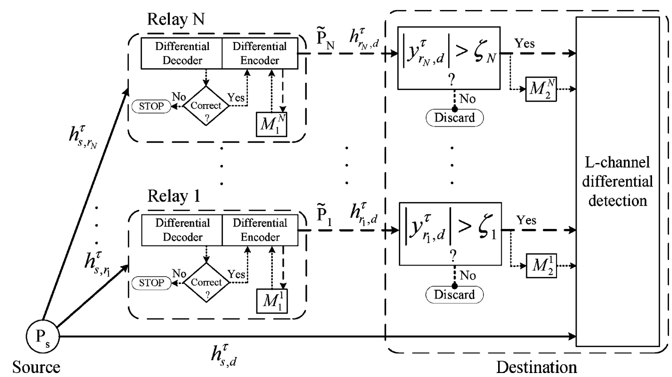

Fig. 2. System descriptions of the multinode differential DF scheme.

The rest of this paper is organized as follows. Section II outlines the DiffAF and the DiffDF schemes for multinode cooperative communications. Section III considers BER analysis for the DiffAF and the DiffDF schemes including BER bounds and their BER approximations. In Section IV, optimum power allocation is determined for the DiffAF scheme where optimum power allocation and optimum threshold are jointly determined for the DiffDF scheme. Simulation results and discussions are given in Section V. Finally, Section VI concludes this paper.

II. Signal Models for Multinode Differential Schemes

We consider a multinode cooperative wireless network with a source and N relays as shown in Fig. 1. Each node can be a source that sends information to its intended destination, or it can be a relay that helps forward information from the source. We consider two differential cooperation strategies, namely, differential amplify-and-forward (DiffAF) and differential decode-and-forward (DiffDF) cooperation schemes. For the DiffAF scheme, each relay amplifies each received signal from the source and then forwards the amplified signal to the destination. In case of the DiffDF scheme (also known as selective forwarding protocol [1]), as in Fig. 2, each relay decodes each received signal and then forwards only correctly decoded symbol to the destination. In order to take advantage of the DiffDF protocol by which only correctly decoded symbol at each relay is forwarded with a certain amount of power to the destination, a decision threshold (ζ_i) is used at the destination to allow only high potential information bearing signal from each of the ith relay link to be combined with that from the direct link before being differentially decoded.

With N cooperative relays in the network, signal transmissions for both DiffAF and DiffDF schemes comprise $N+1$ phases. The first phase belongs to direct transmission, and the rest of N phases is for signal transmission for each of the N relays. The signal models for each of the $N+1$ transmission phases are as follows.

In phase 1, suppose differential M-ary phase shift keying (DMPSK) modulation is used, the modulated information at the source is $v_m = e^{j\phi_m}$, where $\phi_m = 2\pi m/M$ for $m = 0, 1, \ldots, M-1$, and M is the constellation size. The source differentially encodes v_m by $x^\tau = v_m x^{\tau-1}$, where τ is the time index and x^τ is the differentially encoded symbol to be transmitted at time τ. After that, the source transmits x^τ with transmitted power P_s to the destination. Due to the broadcasting nature of the wireless network, the information can also be received by each of the N relays. The corresponding received signals at the destination and the ith relay, for $i = 1, 2, \ldots, N$, can be expressed as

$$y_{s,d}^\tau = \sqrt{P_s} h_{s,d}^\tau x^\tau + \eta_{s,d}^\tau \quad (1)$$

$$y_{s,r_i}^\tau = \sqrt{P_s} h_{s,r_i}^\tau x^\tau + \eta_{s,r_i}^\tau \quad (2)$$

where $h_{s,d}^\tau$ and h_{s,r_i}^τ represent channel coefficients from the source to the destination and from the source to the ith relay, respectively. In this paper, $h_{s,d}^\tau$ and h_{s,r_i}^τ are modeled as complex Gaussian random variables with zero means and variances $\sigma_{s,d}^2$ and σ_{s,r_i}^2, respectively. The terms $\eta_{s,d}^\tau$ and η_{s,r_i}^τ are additive white Gaussian noise at the destination and the ith relay, respectively. Both of these noise terms are modeled as zero-mean complex Gaussian random variables with variance $\mathcal{N}_0$.

In phases 2 to $N+1$, depending on the cooperation protocol under consideration, each of the N relays forwards either the amplified signal or the decoded signal to the destination. Signal models for the DiffAF and the DiffDF schemes in phases 2 to $N+1$ are presented in Section II-A and II-B, respectively.

A. Signal Model for the DiffAF Scheme

For the DiffAF scheme, the received signal in phases 2 to $N+1$ is given by

$$y_{r_i,d}^\tau = \frac{\sqrt{P_i}}{\sqrt{P_s \sigma_{s,r_i}^2 + \mathcal{N}_0}} h_{r_i,d}^\tau y_{s,r_i}^\tau + \eta_{r_i,d}^\tau \quad (3)$$

where P_i represents the transmitted power at the ith relay and $h_{r_i,d}^\tau$ denotes the channel coefficient at time τ at the ith relay-destination link. We model $h_{r_i,d}^\tau$ as a zero-mean complex Gaussian random variable with variance $\sigma_{r_i,d}^2$. In (3), P_i is normalized by $P_s \sigma_{s,r_i}^2 + \mathcal{N}_0$, and hence the ith relay requires only the channel variance between the source and the ith relay (σ_{s,r_i}^2) rather than its instantaneous value. In practice, σ_{s,r_i}^2 can be obtained through long-term averaging of the received signals at the ith relay.

Finally, the received signals from the source and those from all of the relays are combined at the destination, and we have

$$y^{AF} = w_s^{AF} \left(y_{s,d}^{\tau-1}\right)^* y_{s,d}^\tau + \sum_{i=1}^N w_i^{AF} \left(y_{r_i,d}^{\tau-1}\right)^* y_{r_i,d}^\tau \quad (4)$$

where

$$w_s^{AF} = 1/\mathcal{N}_0$$

and

$$w_i^{AF} = (P_s \sigma_{s,r_i}^2 + \mathcal{N}_0)/\mathcal{N}_0(P_s \sigma_{s,r_i}^2 + P_i \sigma_{r_i,d}^2 + \mathcal{N}_0)$$

are used as combining weights for the proposed DiffAF scheme. Here, the channels $\sigma_{r_i,d}^2$ and σ_{s,r_i}^2 are assumed available at the destination. Note that σ_{s,r_i}^2 and $\sigma_{r_i,d}^2$ can be obtained through long-term averaging of the received signals at the ith relay and the destination, respectively. In practice, σ_{s,r_i}^2 can be forwarded from each of the ith relay to the destination over a reliable channel link. Accordingly, without acquiring perfect CSI, the combined signal (4) is differentially decoded by using the detection rule [9]

$$\hat{m} = \arg \max_{m=0,1,\ldots,M-1} \operatorname{Re}\left\{v_m^* y^{AF}\right\}. \quad (5)$$

B. Signal Model for the DiffDF Scheme

In this cooperation system, each relay forwards only correctly decoded symbol to the destination, i.e., $\tilde{P}_i = P_i$ when the ith relay decodes correctly, and $\tilde{P}_i = 0$, otherwise. As shown in Fig. 2, N decision thresholds are used at the destination to allow only high potential information bearing signal from each of the ith relay to be combined with that from the direct link before being differentially decoded.

Specifically, in phases 2 to $N+1$, each of the ith relay differentially decodes the received signal from the source by using the decision rule [9]

$$\hat{m} = \arg \max_{m=0,1,\ldots,M-1} \operatorname{Re}\left\{\left(v_m y_{s,r_i}^{\tau-1}\right)^* y_{s,r_i}^\tau\right\}. \quad (6)$$

Here, we assume an ideal relay that can make judgement on the decoded information whether it is correct or not.[1] If each of the ith relay incorrectly decodes, such incorrectly decoded symbol is discarded. Otherwise, the ith relay differentially re-encodes the information symbol as $\tilde{x}^\tau = v_m \tilde{x}^{\tau-k_i}$, where k_i represents the time index that the ith relay correctly decodes before time τ. Then, $\tilde{x}^\tau$ is forwarded to the destination with transmitted power $\tilde{P}_i = P_i$. After that, $\tilde{x}^\tau$ is stored in a memory, represented by M_1^i in Fig. 2, for subsequent differential encoding. Note that the time index $\tau - k_i$ in $\tilde{x}^{\tau-k_i}$ can be any time before time τ depending on the decoding result in the previous time. The received signal at the destination in phases 2 to $N+1$ can be expressed as

$$y_{r_i,d}^\tau = \begin{cases} \sqrt{P_i} h_{r_i,d}^\tau \tilde{x}^\tau + \eta_{r_i,d}^\tau, & \text{if relay correctly decodes } (\tilde{P}_i = P_i) \\ \eta_{r_i,d}^\tau, & \text{otherwise } (\tilde{P}_i = 0) \end{cases} \quad (7)$$

where $i = 1, 2, \ldots, N$, $h_{r_i,d}^\tau$ denotes the channel coefficient between the ith relay and the destination, and $\eta_{r_i,d}^\tau$ represents an additive noise.

[1]Practically, this can be done at the relay by applying a simple signal-to-noise ratio (SNR) threshold test on the received data [17], [18].

Since the perfect knowledge of CSI is not available at each time instant, the destination does not know when the received signal from the ith relay contains the information. For each ith relay-destination link, a decision threshold ζ_i is used at the destination to make the decision whether to combine $y_{r_i,d}^{\tau}$ with the received signal from the direct link. Specifically, if $|y_{r_i,d}^{\tau}| \leq \zeta_i$ for all i where $|x|$ denotes the absolute value of x, the destination estimates the transmitted symbol based only on the received signal from the direct link. However, if $|y_{r_i,d}^{\tau}| > \zeta_i$ for any i, the received signals from the source and that from the ith relay are combined for joint decoding. In this way, the combined signal at the destination can be written as

$$y^{DF} = w_s^{DF}(y_{s,d}^{\tau-1})^* y_{s,d}^{\tau} + \sum_{i=1}^{N} w_i^{DF} I_{\zeta_i}[|y_{r_i,d}^{\tau}|](y_{r_i,d}^{\tau-l_i})^* y_{r_i,d}^{\tau} \tag{8}$$

where w_s^{DF} and w_i^{DF} are combining weights. In (8), $y_{r_i,d}^{\tau-l_i}$ ($l_i \geq 1$) is the most recent received signal from the ith relay with $|y_{r_i,d}^{\tau-l_i}| > \zeta_i$. It is stored in a memory, represented by M_2^i in Fig. 2, at the destination. The function $I_{\zeta_i}[|y_{r_i,d}^{\tau}|]$ in (8) represents an indicator function in which $I_{\zeta_i}[|y_{r_i,d}^{\tau}|] = 1$ if $|y_{r_i,d}^{\tau}| > \zeta_i$; otherwise, $I_{\zeta_i}[|y_{r_i,d}^{\tau}|] = 0$. After signal combining, the destination jointly differentially decodes the transmitted information by $\hat{m} = \arg\max_{m=0,1,\ldots,M-1} \mathrm{Re}\{v_m^* y^{DF}\}$. Note that using different combining weights (w_s^{DF} and w_i^{DF}) results in different system performances. In this paper, we use $w_s^{DF} = w_i^{DF} = 1/(2\mathcal{N}_0)$, which maximizes the SNR at the combiner output.

III. Performance Analysis for the Multinode Differential Schemes

In this section, BER analysis for the proposed multinode differential cooperation schemes is provided. First, a BER performance for the DiffAF scheme is analyzed. Then, tight BER bounds and simple BER approximations are determined. Finally, a BER analysis for the DiffDF scheme is provided, and its BER lower bound is given.

A. BER Analysis for the DiffAF Scheme

As specified in [14], the BER formulation based on arbitrary combining weights, i.e., w_s^{AF} and w_i^{AF} in (4), is currently not available in the literature. For mathematical tractability, we provide an alternative BER analysis based on optimum combining weights: $\hat{w}_s^{AF} = 1/\mathcal{N}_0$ and $\hat{w}_i^{AF} = (P_s\sigma_{s,r_i}^2 + \mathcal{N}_0)/\mathcal{N}_0(P_s\sigma_{s,r_i}^2 + P_i|h_{r_i,d}^{\tau}|^2 + \mathcal{N}_0)$. The detailed BER derivation can be found in [14] for single relay case, and it is omitted here. Differently from [14], however, in what follows, we provide an alternative closed-form BER formulation, which allows us to analytically calculate optimum power allocation rather than rely on numerical evaluations as presented in [14].

With the optimum combining weights $\hat{w}_s^{AF}$ and $\hat{w}_i^{AF}$, an instantaneous SNR at the combiner output can be written as

$$\gamma^{AF} = \gamma_s^{AF} + \sum_{i=1}^{N} \gamma_i^{AF} \tag{9}$$

where

$$\gamma_s^{AF} \triangleq (P_s|h_{s,d}^{\tau}|^2)/(\mathcal{N}_0)$$

and

$$\gamma_i^{AF} \triangleq (P_s P_i |h_{s,r_i}^{\tau}|^2 |h_{r_i,d}^{\tau}|^2)/(\mathcal{N}_0(P_s\sigma_{s,r_i}^2 + P_i|h_{r_i,d}^{\tau}|^2 + \mathcal{N}_0))$$

. Accordingly, the conditional BER expression for the DiffAF scheme can be approximated by the differential modulation with L-channel diversity receptions [9] as

$$P_{b|\gamma^{AF}}^{AF} \approx \frac{1}{2^{2L}\pi} \int_{-\pi}^{\pi} f(\theta, \beta, L) \exp[-\alpha(\theta)\gamma^{AF}] d\theta \tag{10}$$

where

$$\alpha(\theta) = \frac{b^2(1 + 2\beta\sin\theta + \beta^2)}{2} \tag{11}$$

and

$$f(\theta, \beta, L) = \frac{b^2}{2\alpha(\theta)} \sum_{l=1}^{L} \binom{2L-1}{L-1} \Theta(\beta, \theta, l) \tag{12}$$

in which

$$\Theta(\beta, \theta, l) = \Bigg[(\beta^{-l+1} - \beta^{l+1})\cos\left((l-1)\left(\theta + \frac{\pi}{2}\right)\right) - (\beta^{-l+2} - \beta^{l})\cos\left(l\left(\theta + \frac{\pi}{2}\right)\right)\Bigg].$$

Here, $L = N+1$, and $\beta = a/b$ in which $a = 10^{-3}$ and $b = \sqrt{2}$ for differential binary phase-shift keying (DBPSK) modulation, and $a = \sqrt{2-\sqrt{2}}$ and $b = \sqrt{2+\sqrt{2}}$ for differential quadrature phase-shift keying (DQPSK) modulation [9]. The value of β for higher constellation sizes can be found in [19]. Following the analysis in [14] by using the moment generating function (MGF) method to average the conditional BER (10) over the Rayleigh distributed random variables, we have

$$P_b^{AF} \approx \frac{1}{2^{2(N+1)}\pi} \int_{-\pi}^{\pi} f(\theta, \beta, N+1) \times \mathcal{M}_{\gamma_s^{AF}}(\theta) \prod_{i=1}^{N} \mathcal{M}_{\gamma_i^{AF}}(\theta)\, d\theta \tag{13}$$

where $\mathcal{M}_{\gamma_s^{AF}}(\theta) = 1/(1 + k_{s,d}(\theta))$, in which $k_{s,d}(\theta) \triangleq \alpha(\theta)P_s\sigma_{s,d}^2/\mathcal{N}_0$. The MGF $\mathcal{M}_{\gamma_i^{AF}}(\theta)$ is obtained through double integration of each γ_i^{AF} over two exponential random variables $|h_{s,r_i}|^2$ and $|h_{r_i,d}|^2$. After some manipulations, we have

$$\mathcal{M}_{\gamma_i^{AF}}(\theta) = \frac{1}{1 + k_{s,r_i}(\theta)} \times \left(1 + \frac{k_{s,r_i}(\theta)}{1 + k_{s,r_i}(\theta)} \frac{P_s\sigma_{s,r_i}^2 + \mathcal{N}_0}{P_i} \frac{1}{\sigma_{r_i,d}^2} Z_i(\theta)\right) \tag{14}$$

where

$$Z_i(\theta) = \int_0^\infty \frac{\exp\left(-\frac{u}{\sigma^2_{r_i,d}}\right)}{u+\hat{R}_i(\theta)}du = -e^{R_i(\theta)}\left[\mathcal{E}+\ln R_i(\theta)+\int_0^{R_i(\theta)}\frac{\exp(-t)-1}{t}dt\right] \tag{15}$$

in which $\hat{R}_i(\theta) \triangleq (P_s\sigma^2_{s,r_i}+\mathcal{N}_0)/(P_i[1+k_{s,r_i}(\theta)])$ and $R_i(\theta) \triangleq \hat{R}_i(\theta)/\sigma^2_{r_i,d}$. Note that the last expression in (15) is obtained by applying results from [22, p. 358, eq. (3.352.4); p. 934, eq. (8.212.1)], and $\mathcal{E} \triangleq 0.57721566490\ldots$ represents the Euler's constant. Hence, the average BER is

$$P_b^{AF} \approx \frac{1}{2^{2(N+1)}\pi}\int_{-\pi}^{\pi}\frac{f(\theta,\beta,N+1)}{1+k_{s,d}(\theta)}\prod_{i=1}^{N}\frac{1}{1+k_{s,r_i}(\theta)} \times\left(1+\frac{k_{s,r_i}(\theta)Z_i(\theta)}{1+k_{s,r_i}(\theta)}\frac{P_s\sigma^2_{s,r_i}+\mathcal{N}_0}{P_i\sigma^2_{r_i,d}}\right)d\theta. \tag{16}$$

Using the same technique as in [14], the BER upper bound is obtained by substituting $\theta=\pi/2$ in (11) such that $\alpha(\theta)$ is upper bounded by $\alpha(\theta) \le (b^2(1+\beta)^2)/2$. Hence, the BER upper bound can be obtained by replacing $Z_i(\theta)$ in (16) by $Z_{i,\max}$, and we have

$$P_b^{AF} \lessapprox \frac{1}{2^{2(N+1)}\pi}\int_{-\pi}^{\pi}\frac{f(\theta,\beta,N+1)}{1+k_{s,d}(\theta)}\prod_{i=1}^{N}\frac{1}{1+k_{s,r_i}(\theta)} \times\left(1+\frac{k_{s,r_i}(\theta)Z_{i,\max}}{1+k_{s,r_i}(\theta)}\frac{P_s\sigma^2_{s,r_i}+\mathcal{N}_0}{P_i\sigma^2_{r_i,d}}\right)d\theta \tag{17}$$

where

$$Z_{i,\max} = -e^{R_{i,\min}}\left[\mathcal{E}+\ln R_{i,\min}+\int_0^{R_{i,\min}}\frac{\exp(-t)-1}{t}dt\right] \tag{18}$$

and $R_{i,\min} \triangleq \hat{R}_{i,\min}/\sigma^2_{r_i,d}$ in which $\hat{R}_{i,\min} \triangleq ((P_s\sigma^2_{s,r_i}+\mathcal{N}_0)/P_i)\left[1+P_s\sigma^2_{s,r_i}b^2(1+\beta)^2/2\mathcal{N}_0\right]^{-1}$.

Accordingly, a simple BER upper bound can be obtained by focusing at high SNR region such that all 1's in the denominator of (17) can be discarded. After some manipulations, the simple BER upper bound can be expressed as

$$P_b^{AF} \lessapprox \frac{C(\beta,N+1)\mathcal{N}_0^{N+1}}{P_s\sigma^2_{s,d}} \times\prod_{i=1}^{N}\frac{P_i\sigma^2_{r_i,d}+\left(P_s\sigma^2_{s,r_i}+\mathcal{N}_0\right)Z_{i,\max}}{P_sP_i\sigma^2_{s,r_i}\sigma^2_{r_i,d}} \tag{19}$$

where

$$C(\beta,N+1) = \frac{1}{2^{2(N+1)}\pi}\int_{-\pi}^{\pi}\frac{f(\theta,\beta,N+1)}{\alpha^{N+1}(\theta)}d\theta \tag{20}$$

is a constant that depends on the modulation size and the number of relays, and $\alpha(\theta)$ and $f(\theta,\beta,N+1)$ are specified in (11) and (12), respectively. The BER upper bound (19) reveals that when N relays are available in the network, the DiffAF scheme achieves diversity order of $N+1$ as specified in the exponent of the noise variance.

In case of BER lower bound, we first note that $\alpha(\theta) \ge \alpha(-\pi/2) = (b^2(1-\beta)^2)/2$. By replacing $Z_i(\theta)$ in (16) by $Z_{i,\min}$, we obtain a BER approximation

$$P_b^{AF} \gtrapprox \frac{1}{2^{2(N+1)}\pi}\int_{-\pi}^{\pi}\frac{f(\theta,\beta,N+1)}{1+k_{s,d}(\theta)}\prod_{i=1}^{N}\frac{1}{1+k_{s,r_i}(\theta)} \times\left(1+\frac{k_{s,r_i}(\theta)Z_{i,\min}}{1+k_{s,r_i}(\theta)}\frac{P_s\sigma^2_{s,r_i}+\mathcal{N}_0}{P_i\sigma^2_{r_i,d}}\right)d\theta \tag{21}$$

where

$$Z_{i,\min} = -e^{R_{i,\max}}\left[\mathcal{E}+\ln R_{i,\max}+\int_0^{R_{i,\max}}\frac{\exp(-t)-1}{t}dt\right] \tag{22}$$

and

$$R_{i,\max} \triangleq \hat{R}_{i,\max}/\sigma^2_{r_i,d}$$

in which

$$\hat{R}_{i,\max} \triangleq ((P_s\sigma^2_{s,r_i}+\mathcal{N}_0)/P_i)\left[1+P_s\sigma^2_{s,r_i}b^2(1-\beta)^2/2\mathcal{N}_0\right]^{-1}$$

. Furthermore, by ignoring all 1's in the denominator of (21), we obtain a simple BER approximation

$$P_b^{AF} \approx \frac{C(\beta,N+1)\mathcal{N}_0^{N+1}}{P_s\sigma^2_{s,d}} \times\prod_{i=1}^{N}\frac{P_i\sigma^2_{r_i,d}+\left(P_s\sigma^2_{s,r_i}+\mathcal{N}_0\right)Z_{i,\min}}{P_sP_i\sigma^2_{s,r_i}\sigma^2_{r_i,d}} \tag{23}$$

where $C(\beta,N+1)$ and $Z_{i,\min}$ are specified in (20) and (22), respectively. We can see from the exponent of the noise variance in (23) that the achievable diversity order is $N+1$. As will be shown in the simulation results, these two BER approximations are tight at high SNR region.

B. BER Analysis for the DiffDF Scheme

BER analysis of the DiffDF scheme, as described in Section II-B, is considered in this section. First, different SNR scenarios are characterized according to the received signal $y^{\tau}_{r_i,d}$, threshold ζ_i, and memories M_1^i and M_2^i. Then, probability of occurrence is provided for each of these SNR scenarios. After that, average BER is derived based on the probability of occurrence and the combined SNR for each scenario. Finally, a tractable BER lower bound is provided at the end of this section.

1) Characterization of Different SNR Scenarios: At the destination, different combined SNRs may occur according to a comparison the received signal $(y^{\tau}_{r_i,d})$ and the threshold (ζ_i) as well as the signals stored in memory M_1^i and M_2^i. In this way, the destination encounters six possible SNR scenarios at each relay-destination link, and we characterize each of them as follows. For a given network state j, we denote s_j^i as an integer number that represents an SNR scenario at the ith relay-destination link, i.e., $s_j^i \in \{1,2,3,4,5,6\}$. A set of joint event $\Phi^i_{s_j^i}$ for

$i = 1, 2, \ldots, N$ will be related to each of the scenario s_j^i. Specifically, when $s_j^i = 1$, $\Phi_1^i \triangleq \left\{|y_{r_i,d}^\tau| \le \zeta_i\right\}$ represents a joint event that received signals from the ith relay link is not greater than the thresholds. We characterize $\Phi_2^i \triangleq \{|y_{r_i,d}^\tau| > \zeta_i, \tilde{P}_i^\tau = P_i, \tilde{P}_i^{\tau-l_i} = P_i, l_i = k_i\}$ as a joint event including $|y_{r_i,d}^\tau| > \zeta_i$, where the relay correctly decodes at time τ and $\tau - l_i$ and the information symbols at time k_i and l_i in memories M_1^i and M_2^i are the same. The rest scenarios are $\Phi_3^i \triangleq \{|y_{r_i,d}^\tau| > \zeta_i, \tilde{P}_i^\tau = P_i, \tilde{P}_i^{\tau-l_i} = P_i, l_i \ne k_i\}$, $\Phi_4^i \triangleq \{|y_{r_i,d}^\tau| > \zeta_i, \tilde{P}_i^\tau = P_i, \tilde{P}_i^{\tau-l_i} = 0\}$, $\Phi_5^i \triangleq \{|y_{r_i,d}^\tau| > \zeta_i, \tilde{P}_i^\tau = 0, \tilde{P}_i^{\tau-l_i} = P_i\}$, and $\Phi_6^i \triangleq \{|y_{r_i,d}^\tau| > \zeta_i, \tilde{P}_i^\tau = 0, \tilde{P}_i^{\tau-l_i} = 0\}$. They are interpreted in a similar way as that of Φ_2^i.

2) Probability of Occurrence for Each SNR Scenario: To determine probability of occurrence for each scenario, we first find that the probability that the ith relay forwards information with transmitted power $\tilde{P}_i = 0$ due to incorrect decoding is related to the symbol error rate of DMPSK modulation as [21]

$$\Psi(\gamma_{s,r_i}^{DF}) = \frac{1}{\pi}\int_0^{(M-1)\pi/M} \exp\left[-g(\phi)\gamma_{s,r_i}^{DF}\right] d\phi \tag{24}$$

where $\gamma_{s,r_i}^{DF} = P_s|h_{s,r_i}^\tau|^2/\mathcal{N}_0$ represents an instantaneous SNR at the ith relay, and $g(\phi) = \sin^2(\pi/M)/(1+\cos(\pi/M)\cos(\phi))$. Accordingly, the probability of correct decoding at the ith relay (or probability of forwarding with transmitted power $\tilde{P}_i = P_i$) is $1 - \Psi(\gamma_{s,r_i}^{DF})$. Therefore, the chance that Φ_1^i occurs is determined by the weighted sum of conditional probabilities given that $\tilde{P}_i = P_i$ or 0, and we have

$$\begin{aligned} P_r^{h,DF}(\Phi_1^i) &= P_r^{h,DF}\left(|y_{r_i,d}^\tau| \le \zeta_i \mid \tilde{P}_i^\tau = 0\right)\Psi(\gamma_{s,r_i}^\tau) \\ &\quad + P_r^{h,DF}\left(|y_{r_i,d}^\tau| \le \zeta_i \mid \tilde{P}_i^\tau = P_i\right)\left[1 - \Psi(\gamma_{s,r_i}^\tau)\right] \\ &= \left(1 - \exp\left(\frac{-\zeta_i^2}{\mathcal{N}_0}\right)\right)\Psi(\gamma_{s,r_i}^\tau) \\ &\quad + \left(1 - \mathcal{M}\left(P_i|h_{r_i,d}^\tau|^2, \zeta_i\right)\right)\left[1 - \Psi(\gamma_{s,r_i}^\tau)\right] \end{aligned} \tag{25}$$

where the second equality is obtained by substituting $P_r^{h,DF}(|y_{r_i,d}^\tau| \le \zeta_i \mid \tilde{P}_i^\tau = 0) = 1 - \exp(-\zeta_i^2/\mathcal{N}_0)$, which is related to cumulative distribution function (CDF) of a Rayleigh-distributed random variable. The term $P_r^{h,DF}\left(|y_{r_i,d}^\tau| \le \zeta_i \mid \tilde{P}_i^\tau = P_i\right)$ is related to the CDF of Rician-distributed random variable such that $P_r^{h,DF}\left(|y_{r_i,d}^\tau| \le \zeta_i \mid \tilde{P}_i^\tau = P_i\right) = 1 - \mathcal{M}\left(P_i|h_{r_i,d}^\tau|^2, \zeta_i\right)$, where

$$\mathcal{M}\left(P_i|h_{r_i,d}^\tau|^2, \zeta_i\right) \triangleq Q_1\left(\sqrt{\frac{P_i|h_{r_i,d}^\tau|^2}{(\mathcal{N}_0/2)}}, \frac{\zeta_i}{\sqrt{\mathcal{N}_0/2}}\right) \tag{26}$$

in which $Q_1(\alpha, \beta)$ is the Marcum Q-function [9].

According to the definition of each SNR scenario in Section III-B1, a chance that each of the scenarios Φ_2 to Φ_6 happens is conditioned on an event that $|y_{r_i,d}^{\tau-l_i}| > \zeta_i$. Since the events at time $\tau - l_i$ and time τ are independent, then the probability that Φ_2^i occurs is given by

$$\begin{aligned} P_r^{h,DF}(\Phi_2^i) &= P_r^{h,DF}\left(|y_{r_i,d}^\tau| > \zeta_i, \tilde{P}_i^\tau = P_i\right) \\ &\quad \times P_r^{h,DF}\left(\tilde{P}_i^{\tau-l_i} = P_i, l_i = k_i \,\middle|\, |y_{r_i,d}^{\tau-l_i}| > \zeta_i\right) \\ &\approx \frac{\mathcal{M}^2\left(P_i|h_{r_i,d}^\tau|^2, \zeta_i\right)\left(1 - \Psi(\gamma_{s,r_i}^\tau)\right)^2}{1 - (1 - e^{-\zeta_i^2/\mathcal{N}_0})\Psi(\gamma_{s,r_i}^\tau)}. \end{aligned} \tag{27}$$

The approximation in (27) is obtained by using the result in (24) and the fact that $P_r^{h,DF}\left(|y_{r_i,d}^\tau| > \zeta_i \mid \tilde{P}_i^\tau = P_i\right) = \mathcal{M}\left(P_i|h_{r_i,d}^\tau|^2, \zeta_i\right)$. In this way, the first term in (27) can be calculated as $P_r^{h,DF}\left(|y_{r_i,d}^\tau| > \zeta_i, \tilde{P}_i^\tau = P_i\right) = \mathcal{M}\left(P_i|h_{r_i,d}^\tau|^2, \zeta_i\right)\left(1 - \Psi(\gamma_{s,r_i}^\tau)\right)$. In addition, the second term in (27) can be approximated by using the concept of conditional probability and applying Bayes' rule such that

$$\begin{aligned} &P_r^{h,DF}\left(\tilde{P}_i^{\tau-l_i} = P_i, l_i = k_i \mid |y_{r_i,d}^{\tau-l_i}| > \zeta_i\right) \\ &\qquad \approx \frac{\left(\mathcal{M}\left(P_i|h_{r_i,d}^\tau|^2, \zeta_i\right)\left(1 - \Psi(\gamma_{s,r_i}^\tau)\right)\right)}{\left(1 - (1 - e^{-\zeta_i^2/\mathcal{N}_0})\Psi(\gamma_{s,r_i}^\tau)\right)}. \end{aligned}$$

Next, the chance that the scenario Φ_3^i happens can be written as

$$P_r^{h,DF}(\Phi_3^i) = P_r^{h,DF}(\Phi_2^i \cup \Phi_3^i) - P_r^{h,DF}(\Phi_2^i) \tag{28}$$

where

$$\begin{aligned} &P_r^{h,DF}(\Phi_2^i \cup \Phi_3^i) \\ &\quad \triangleq P_r^{h,DF}\left(|y_{r_i,d}^\tau| > \zeta_i, \tilde{P}_i^\tau = P_i, \tilde{P}_i^{\tau-l_i} = P_i, \middle| |y_{r_i,d}^{\tau-l_i}| > \zeta_i\right) \\ &\quad = P_r^{h,DF}\left(|y_{r_i,d}^\tau| > \zeta_i, \tilde{P}_i^\tau = P_i\right) \\ &\qquad \times \frac{P_r^{h,DF}\left(|y_{r_i,d}^{\tau-l_i}| > \zeta_i, \tilde{P}_i^{\tau-l_i} = P_i\right)}{P_r^{h,DF}\left(|y_{r_i,d}^{\tau-l_i}| > \zeta_i\right)}. \end{aligned} \tag{29}$$

Substituting (27) and (29) into (28), after some manipulations, we have

$$\begin{aligned} &P_r^{h,DF}(\Phi_3^i) \\ &\quad = \mathcal{M}^2\left(P_i|h_{r_i,d}^\tau|^2, \zeta_i\right) \\ &\qquad \times \left(\frac{1}{\Gamma(P_s|h_{s,r_i}^\tau|^2, P_i|h_{r_i,d}^\tau|^2)} \right. \\ &\qquad\quad \left. - \frac{1}{\left(1 - (1 - e^{-\zeta_i^2/\mathcal{N}_0})\Psi(\gamma_{s,r_i}^\tau)\right)}\right)\left(1 - \Psi(\gamma_{s,r_i}^\tau)\right)^2 \end{aligned} \tag{30}$$

in which $\Gamma(P_s|h_{s,r_i}^{\tau-l_i}|^2, P_i|h_{r_i,d}^{\tau-l_i}|^2)$ is defined as an expression that results from applying the concept of total probability [23] to $P_r^{h,DF}\left(|y_{r_i,d}^{\tau-l_i}| > \zeta_i\right)$

$$\begin{aligned} P_r^{h,DF}\left(|y_{r_i,d}^{\tau-l_i}| > \zeta_i\right) &= \mathcal{M}\left(P_i|h_{r_i,d}^{\tau-l_i}|^2, \zeta_i\right)\left(1 - \Psi(\gamma_{s,r_i}^{\tau-l_i})\right) \\ &\quad + e^{-\zeta_i^2/\mathcal{N}_0}\Psi(\gamma_{s,r_i}^{\tau-l_i}) \\ &\triangleq \Gamma(P_s|h_{s,r_i}^{\tau-l_i}|^2, P_i|h_{r_i,d}^{\tau-l_i}|^2). \end{aligned} \tag{31}$$

With the assumption of almost constant channels at time τ and $\tau - l_i$, we have $P_r^{h,DF}(\Phi_4^i) = P_r^{h,DF}(\Phi_5^i)$, i.e., scenarios Φ_4^i and

Φ_5^i occur with the same probability. Following the calculation steps as used in (29), we have

$$\begin{aligned} P_r^{h,DF}(\Phi_4^i) &= P_r^{h,DF}(\Phi_5^i) \\ &= \frac{\mathcal{M}\left(P_i|h_{r_i,d}^\tau|^2,\zeta_i\right)e^{(-\zeta_i^2/\mathcal{N}_0)}\Psi(\gamma_{s,r_i}^\tau)\left(1-\Psi(\gamma_{s,r_i}^\tau)\right)}{\Gamma(P_s|h_{s,r_i}^\tau|^2,P_i|h_{r_i,d}^\tau|^2)}. \end{aligned} \tag{32}$$

Finally, the chance that scenario Φ_6^i occurs can be determined as

$$\begin{aligned} P_r^{h,DF}(\Phi_6^i) &= \frac{P_r^{h,DF}\left(|y_{r_i,d}^\tau|>\zeta_i,\tilde{P}_i^\tau=0\right)P_r^{h,DF}\left(|y_{r_i,d}^{\tau-l_i}|>\zeta_i,\tilde{P}_i^{\tau-l_i}=0\right)}{P_r^{h,DF}\left(|y_{r_i,d}^{\tau-l_i}|>\zeta_i\right)} \\ &= e^{-2\zeta_i^2/\mathcal{N}_0}\Psi(\gamma_{s,r_i}^\tau)\left(\frac{1}{\Gamma(P_s|h_{s,r_i}^\tau|^2,P_i|h_{r_i,d}^\tau|^2)}\right). \end{aligned} \tag{33}$$

3) Approximate BER Expression for the DiffDF Scheme: We know from Section III-B1 that each relay contributes six possible SNR scenarios at the destination. For a network with N relays, there are totally 6^N numbers of network states. We denote $S_j \triangleq [s_j^1\ s_j^2\ \ldots\ s_j^N]$ as an $1\times N$ matrix of a network state j, where $s_j^i \in \{1,2,\ldots,6\}$. Accordingly, the average BER can be expressed as

$$P_b^{DF} = E\left[P_b^{h,DF}\right] = \sum_{j=1}^{6^N} E\left[\left(P_b^{h,DF}|_{S_j}\right)\prod_{i=1}^{N} P_r^{h,DF}(\Phi_{s_j^i}^i)\right] \tag{34}$$

where $P_r^{h,DF}(\Phi_{s_j^i}^i)$ for each s_j^i is specified in (25)–(33), $P_b^{h,DF}|_{S_j}$ represents a conditional BER for a given S_j, and $E[\cdot]$ denotes the expectation operator.

Because it is difficult to find a closed-form solution for the BER in (34), we further simplify (34) by separating a set of all possible network states, denoted by $\mathbb{S}$, into two disjoint subsets as $\mathbb{S} = \mathbb{S}^{1,2} \cup (\mathbb{S}^{1,2})^c$, where $\mathbb{S}^{1,2}$ denotes all possible network states that every element in the network state S_j is either one or two, and $(\mathbb{S}^{1,2})^c$ denotes the remaining possible network states. Note that the cardinality of $\mathbb{S}^{1,2}$ and $(\mathbb{S}^{1,2})^c$ is $|\mathbb{S}^{1,2}| = 2^N$ and $|(\mathbb{S}^{1,2})^c| = 6^N - 2^N$, respectively. In this way, we can express the average BER (34) as

$$\begin{aligned} P_b^{DF} &= \sum_{j=1}^{2^N} E\left[\left(P_b^{h,DF}|_{S_j\in\mathbb{S}^{1,2}}\right)\prod_{i=1}^{N} P_r^{h,DF}(s_j^i)\right] \\ &\quad + \sum_{j=1}^{6^N-2^N} E\left[\left(P_b^{h,DF}|_{S_j\in(\mathbb{S}^{1,2})^c}\right)\prod_{i=1}^{N} P_r^{h,DF}(s_j^i)\right] \\ &\triangleq P_{b,1}^{DF} + P_{b,2}^{DF}. \end{aligned} \tag{35}$$

The first term in the right-hand side of (35), $P_{b,1}^{DF}$, results from the cases where every element in the network state S_j is either one or two; the second term $P_{b,2}^{DF}$ results from the remaining cases. These two terms can be determined as follows.

First, for notational convenience, let us denote $L(S_j)$ as the number of combining branches. By definition, we can express $L(S_j)$ as

$$L(S_j) = \sum_{i=1}^{N} \hat{L}(s_j^i) + 1 \tag{36}$$

where $\hat{L}(s_j^i) = 0$ when $s_j^i = 1$, and $\hat{L}(s_j^i) = 1$, otherwise. Note that the addition of 1 in (36) corresponds to the contribution of signal from the direct link.

Next, consider the case that every element in the network state S_j is either one or two, then the conditional BER $P_b^{h,DF}|_{S_j\in\mathbb{S}^{1,2}}$ can be obtained from the multibranch differential detection of DMPSK signals as [9]

$$\begin{aligned} P_b^{h,DF}|_{S_j\in\mathbb{S}^{1,2}} &= \frac{1}{2^{2L(S_j)}\pi}\int_{-\pi}^{\pi} f\left(\theta,\beta,L(S_j)\right)\exp\left[-\alpha(\theta)\gamma_{S_j\in\mathbb{S}^{1,2}}^{DF}\right]d\theta \\ &\triangleq \Lambda(\gamma_{S_j\in\mathbb{S}^{1,2}}^{DF}) \end{aligned} \tag{37}$$

in which $\alpha(\theta)$ and $f(\theta,\beta,L(S_j))$ are specified in (11) and (12), respectively. The term $\gamma_{S_j\in\mathbb{S}^{1,2}}^{DF}$ is the SNR at the combined output, which is given by

$$\gamma_{S_j\in\mathbb{S}^{1,2}}^{DF} = \frac{P_s|h_{s,d}^\tau|^2}{\mathcal{N}_0} + \sum_{i=1}^{N}\frac{(s_j^i-1)P_i|h_{r_i,d}^\tau|^2}{\mathcal{N}_0}, \qquad s_j^i\in\{1,2\}. \tag{38}$$

Then, the conditional BER $P_b^{h,DF}|_{S_j\in(\mathbb{S}^{1,2})^c}$ for the remaining cases can be found as follows. Since up to now the conditional BER formulation for DMPSK with arbitrary-weighted combining has not been available in the literature, $P_b^{h,DF}|_{S_j\in(\mathbb{S}^{1,2})^c}$ cannot be exactly determined. For analytical tractability of the analysis, we resort to an approximate BER, in which the signal from the relay i is considered as noise when any scenario from Φ_3^i to Φ_6^i occurs. As we will show in the succeeding section, the analytical BER obtained from this approximation is close to the simulation results. The conditional BER for these cases can be approximated as $P_b^{h,DF}|_{S_j\in(\mathbb{S}^{1,2})^c} \approx \Lambda(\gamma_{S_j\in(\mathbb{S}^{1,2})^c}^{DF})$, where

$$\gamma_{S_j\in(\mathbb{S}^{1,2})^c}^{DF} = \frac{P_s|h_{s,d}^\tau|^2 + \sum_{i=1}^{N} I_2[s_j^i]P_i|h_{r_i,d}^\tau|^2}{\mathcal{N}_0+\hat{\mathcal{N}_0}}, \qquad s_j^i\in\{1,2,\ldots,6\} \quad \forall i \tag{39}$$

in which

$$\hat{\mathcal{N}_0} \triangleq \frac{\sum_{i=1}^{N}(1-I_2[s_j^i])\mathcal{N}_{s_j^i}}{\frac{P_s|h_{s,d}^\tau|^2}{\mathcal{N}_0} + \sum_{i=1}^{N} I[s_j^i]P_i|h_{r_i,d}^\tau|^2\mathcal{N}_0}$$

and $\mathcal{N}_{s_j^i}$ depends on s_j^i as follows: $\mathcal{N}_{s_j^i} = (P_i|h_{r_i,d}^\tau|^2 + \mathcal{N}_0)^2/\mathcal{N}_0$ when $s_j^i = 2$, $\mathcal{N}_{s_j^i} = P_i|h_{r_i,d}^\tau|^2 + \mathcal{N}_0$ when $s_j^i = 3,4,5$, and $\mathcal{N}_{s_j^i} = \mathcal{N}_0$ when $s_j^i = 6$. In (39), $I_2[s_j^i]$ is defined as an indicator function based on the occurrence of s_j^i such that $I_2[s_j^i] = 1$ when $s_j^i = 2$, and $I_2[s_j^i] = 0$ when $s_j^i = 1,3,4,5,6$.

From the previous results, $P_{b,2}^{DF}$ in (35) can be approximated as

$$P_{b,2}^{DF} \approx \sum_{j=1}^{6^N-2^N} \frac{1}{4^{L(S_j)}\pi} \int_{-\pi}^{\pi} f(\theta,\beta,L(S_j)) \times E\left[e^{\left(-\alpha(\theta)\gamma^{DF}_{S_j\in(\mathbb{S}^{1,2})^c}\right)} \prod_{i=1}^{N} P_r^{h,DF}(s_j^i) \right] d\theta \quad (40)$$

where

$$E\left[e^{\left(-\alpha(\theta)\gamma^{DF}_{S_j\in(\mathbb{S}^{1,2})^c}\right)} \prod_{i=1}^{N} P_r^{h,DF}(s_j^i) \right] = \underbrace{\int\cdots\int}_{2N+1 \text{ folds}} \exp\left(-\alpha(\theta)\gamma^{DF}_{S_j\in(\mathbb{S}^{1,2})^c}\right) \times \prod_{i=1}^{N} P_r^{h,DF}(s_j^i) f(\varepsilon_1) f(\varepsilon_2)\cdots f(\varepsilon_{2N+1}) \times d\varepsilon_1 d\varepsilon_2 \cdots d\varepsilon_{2N+1} \quad (41)$$

in which $\gamma^{DF}_{S_j\in(\mathbb{S}^{1,2})^c}$ is given in (39), and $\prod_{i=1}^{N} P_r^{h,DF}(s_j^i)$ is calculated by using (25)–(33). We can see from (40) that the evaluation of $P_{b,2}^{DF}$ involves at most $(2N+2)$-fold integration. Although $P_{b,2}^{DF}$ can be numerically determined, the calculation time is prohibitively long even for a cooperation system with small number of relays.

Now, we determine $P_{b,1}^{DF}$ in (35) as follows. The term $\prod_{i=1}^{N} P_r^{h,DF}(s_j^i)$ is a product of probabilities of occurrence of scenarios 1 and 2, and it can be expressed as

$$\prod_{i=1}^{N} P_r^{h,DF}(s_j^i) = \prod_{i=1}^{N} \left[(2-s_j^i)P_r^{h,DF}(\Phi_1^i) + (s_j^i-1)P_r^{h,DF}(\Phi_2^i)\right]. \quad (42)$$

Substitute (37), (38), and (42) into the expression of $P_{b,1}^{DF}$ in (35), and then average over all CSIs, resulting in

$$P_{b,1}^{DF} \approx \sum_{j=1}^{2^N} \left(\frac{1}{2^{2L(S_j)}\pi}\right) \int_{-\pi}^{\pi} \left(\frac{f(\theta,\beta,L(S_j))}{1+\frac{\alpha(\theta)P_s\sigma_{s,d}^2}{\mathcal{N}_0}} \right) \times \prod_{i=1}^{N} \left[(2-s_j^i)X + (s_j^i-1)Y\right] d\theta \quad (43)$$

where we denote $X \triangleq E\left[P_r^{h,DF}(\Phi_1^i)\right]$, which can be determined as

$$X = (1-e^{-\zeta_i^2/\mathcal{N}_0}) G\left(1+\frac{g(\phi)P_s\sigma_{s,r_i}^2}{\mathcal{N}_0}\right) + \left(1-\int_0^\infty \frac{\mathcal{M}(P_i q,\zeta_i)}{\sigma_{r_i,d}^2} e^{-q/\sigma_{r_i,d}^2} dq\right) \times \left(1-G\left(1+\frac{g(\phi)P_s\sigma_{s,r_i}^2}{\mathcal{N}_0}\right)\right) \quad (44)$$

in which $G(c(\phi)) \triangleq (1/\pi)\int_0^{(M-1)\pi/M}[c(\phi)]^{-1}d\phi$, and $Y \triangleq E[\exp(-\alpha(\theta)P_i|h_{r_i,d}^\tau|^2/\mathcal{N}_0)\cdot P_r^{h,DF}(\Phi_2^i)]$, which can be approximated as

$$Y \approx \frac{1}{\sigma_{s,r_i}^2\sigma_{r_i,d}^2} \int_0^\infty \int_0^\infty \frac{\mathcal{M}^2(P_i q,\zeta_i)\left(1-\Psi\left(\frac{P_s u}{\mathcal{N}_0}\right)\right)^2}{1-(1-e^{-\zeta_i^2/\mathcal{N}_0})\Psi\left(\frac{P_s u}{\mathcal{N}_0}\right)} \times e^{-(\alpha(\theta)(P_i/\mathcal{N}_0)+1/\sigma_{r_i,d}^2)q} e^{-u/\sigma_{s,r_i}^2} dq\, du. \quad (45)$$

Substituting (40) and (43) into (35), we finally obtain the average BER of the multinode DiffDF scheme.

To get more insightful understanding, we further determine a BER lower bound of the multinode DiffDF scheme as follows. Since the exact BER formulations under the scenarios Φ_4^i, Φ_5^i, and Φ_6^i are currently unavailable, and the chances that these three scenarios happen are small at high SNR, we lower bound the BER from these scenarios by zero. Also, we lower bound the BER under the scenario Φ_3^i by that under Φ_2^i; this allows us to express the lower bound in terms of $P_r^h(\Phi_2^i \cup \Phi_3^i)$ (instead of $P_r^h(\Phi_3^i)$ or $P_r^h(\Phi_2^i)$), which can be obtain without any approximation. In this way, the BER of multinode DiffDF scheme can be lower bounded by

$$P_b^{lb,DF} \approx \sum_{j=1}^{2^N} \left(\frac{1}{2^{2L(S_j)}\pi}\right) \int_{-\pi}^{\pi} \left(\frac{f(\theta,\beta,L(S_j))}{1+\frac{\alpha(\theta)P_s\sigma_{s,d}^2}{\mathcal{N}_0}} \right) \times \prod_{i=1}^{N} \left[(2-s_j^i)X + (s_j^i-1)\hat{Y}\right] d\theta \quad (46)$$

where X is given in (44) and

$$\hat{Y} \triangleq E\left[\exp\left(-\frac{\alpha(\theta)P_i|h_{r_i,d}^\tau|^2}{\mathcal{N}_0}\right)\cdot P_r^{h,DF}(\Phi_2^i\cup\Phi_3^i)\right] = \frac{1}{\sigma_{s,r_i}^2}\int_0^\infty s(u,\theta) e^{-u/\sigma_{s,r_i}^2} du \quad (47)$$

in which

$$s(u,\theta) \triangleq \int_0^\infty \frac{\mathcal{M}^2(P_i q,\zeta_i)\left(1-\Psi\left(\frac{P_s u}{\mathcal{N}_0}\right)\right)^2}{\sigma_{r_i,d}^2\Gamma(P_s u, P_i q)} \times \exp\left(-\left(\alpha(\theta)\frac{P_i}{\mathcal{N}_0}+\frac{1}{\sigma_{r_i,d}^2}\right)q\right) dq. \quad (48)$$

We will show through numerical evaluation that the BER lower bound (46) is very close to the simulated performance.

IV. Performance Enhancement by Optimizing Threshold and Power Allocation

In this section, we provide optimum power allocation for the proposed DiffAF/DiffDF cooperation schemes. First, optimum power allocation for the DiffAF scheme is presented. With some approximations on the obtained BER expression, we are able to obtain a closed-form optimum power allocation for the DiffAF scheme. Then, we jointly determine the optimum threshold and optimum power allocation for the DiffDF scheme. Numerical results and discussions are provided.

A. Optimum Power Allocation for the DiffAF Scheme

We formulate an optimization problem to minimize the BER under a fixed total transmitted power $P = P_s + \sum_{i=1}^{N} P_i$. Based on the simple BER approximation (23), the optimization problem can be formulated as (49), shown at the bottom of the page. Although (49) can be solved numerically, it is difficult to get some insights. To further simplify the problem, we consider a high-SNR scenario where $\hat{R}_{i,\max}$ can be approximated as $\hat{R}_{i,\max} \approx (2\mathcal{N}_0)/(b^2(1-\beta)^2 P_i)$. Then, we can rewrite $Z_{i,\min}$ in (22) as

$$Z_{i,\min} \approx \int_0^{\infty} \frac{\exp\left(-\frac{u}{\sigma_{r_i,d}^2}\right)}{u + \frac{2\mathcal{N}_0}{(b^2(1-\beta)^2 P_s c_i)}} du = -e^{B_{c_i}} \left[\mathcal{E} + \ln B_{c_i} + \int_0^{B_{c_i}} \frac{\exp(-t)-1}{t} dt\right] \quad (50)$$

where $c_i = P_i/P_s$ and $B_{c_i} \triangleq \hat{B}_{c_i}/\sigma_{r_i,d}^2$ in which $\hat{B}_{c_i} = 2\mathcal{N}_0/(b^2(1-\beta)^2 P_s c_i)$. Since the integration term in the last expression of (50) is small compared to $\mathcal{E} + \ln B_{c_i}$, it can be neglected without significant effect on the power allocation. Hence, $Z_{i,\min}$ can be further approximated by

$$Z_{i,\min} \approx -e^{B_{c_i}} \left(\mathcal{E} + \ln B_{c_i}\right). \quad (51)$$

As will be shown later, the obtained optimum power allocation based on the approximated $Z_{i,\min}$ in (51) yields almost the same performance as that with exact $Z_{i,\min}$ as specified in (22).

Substituting (51) into (49), the optimization problem can be simplified to (52), shown at the bottom of the page. Optimizing (52) by using the Lagrangian method as given in the Appendix, the optimum solution of (52) can be obtained by finding c_i that satisfies

$$(N+1)q - \frac{1}{c_i} - Q(c_i,q) + \frac{\sigma_{r_i,d}^2 + \sigma_{s,r_i}^2 \left[\frac{\Upsilon}{Pqc_i^2} e^{B_{c_i}} \left(\mathcal{E} + \ln B_{c_i}\right) + \frac{e^{B_{c_i}}}{c_i}\right]}{c_i \sigma_{r_i,d}^2 - \sigma_{s,r_i}^2 e^{B_{c_i}} \left(\mathcal{E} + \ln B_{c_i}\right)} = 0 \quad (53)$$

in which

$$Q(c_i,q) \triangleq \left(\frac{1}{P}\right) \sum_{i=1}^{N} \frac{\sigma_{s,r_i}^2 \Upsilon e^{B_{c_i}} \left(\mathcal{E} + \ln B_{c_i} + \frac{1}{B_{c_i}}\right)}{c_i \left[c_i \sigma_{r_i,d}^2 - \sigma_{s,r_i}^2 e^{B_{c_i}} \left(\mathcal{E} + \ln B_{c_i}\right)\right]}.$$

Given a specific $q \triangleq P_s/P$ for $q \in (0,1)$, we can find the corresponding c_i, denoted by $c_i(q)$, that satisfies (53). The optimum power allocation can then be obtained by finding $q = \hat{q}$ that satisfies

$$1 + \sum_{i=1}^{N} c_i(\hat{q}) - \frac{1}{\hat{q}} = 0. \quad (54)$$

The resulting optimum power allocation for the source is $a_s = \hat{q}$. Since $c_i(\hat{q}) = P_i/P_s = a_i/\hat{q}$, then the optimum power allocation for each of the ith relay is $a_i = \hat{q} c_i(\hat{q})$ for $i = 1, 2, \ldots, N$.

1) Optimum Power Allocation for Single-Relay Systems: For single relay systems, the optimization problems (A-5) and (54) are reduced to finding q such that

$$(N+1)q - \frac{1}{c_1} + \frac{\sigma_{r_1,d}^2 + \sigma_{s,r_1}^2 \Upsilon e^{B_{c_1}} \left[\frac{1}{Pq}\left(\mathcal{E} + \ln B_{c_1}\right) + \frac{1}{B_{c_1}}\right]}{c_1^2 [c_1 \sigma_{r_1,d}^2 - \sigma_{s,r_1}^2 e^{B_{c_1}} \left(\mathcal{E} + \ln B_{c_1}\right)]} - \frac{1}{P} \frac{\sigma_{s,r_1}^2 \Upsilon e^{B_{c_1}} \left(\mathcal{E} + \ln B_{c_1} + \frac{1}{B_{c_1}}\right)}{c_1 \left[c_1 \sigma_{r_1,d}^2 - \sigma_{s,r_1}^2 e^{B_{c_1}} (\mathcal{E} + \ln B_{c_1})\right]} = 0$$

and

$$1 + c_1(q) - \frac{1}{q} = 0 \quad (55)$$

which can be simply solved by any single-dimensional search techniques. In this way, the complexity of the optimization problem can be greatly reduced, while the resulting optimum power allocation is close to that from exhaustive search in [14]. For example, Table I compares optimum power allocation from the exhaustive search in [14] and that from solving the low-complexity optimization problem in (55). The results in Table I are obtained at reasonable high SNR region, e.g., 20 or 30 dB. The DBPSK or DQPSK modulations are used, and $\left[\sigma_{s,d}^2, \sigma_{s,r_i}^2, \sigma_{r_i,d}^2\right]$ represents a vector containing channel variances of the source-destination link, the source-relay link, and the relay-destination link, respectively. We can see from the table that the optimum power allocation based on (55) is very close to that from the numerical search, for any relay location. There is only about 1%–2% difference in the obtained results between these two methods.

2) Optimum Power Allocation for Multirelay Systems: For multirelay systems, (A-5) and (54) can be used to find the optimum power allocation. Nevertheless, the optimization based on (A-5) and (54) involves $(N+1)$-dimensional search because

$$\arg \min_{P_s, \{P_i\}_{i=1}^N} \left\{ \frac{C(\beta, N+1)\mathcal{N}_0^{N+1}}{P_s \sigma_{s,d}^2} \prod_{i=1}^{N} \frac{P_i \sigma_{r_i,d}^2 + (P_s \sigma_{s,r_i}^2 + \mathcal{N}_0) Z_{i,\min}}{P_s P_i \sigma_{s,r_i}^2 \sigma_{r_i,d}^2} \right\}, \text{ subject to } P_s + \sum_{i=1}^{N} P_i \leq P, \quad P_i \geq 0 \quad \forall i. \quad (49)$$

$$\arg \min_{P_s, \{P_i\}_{i=1}^N} \left\{ \frac{1}{P_s^{N+1}} \prod_{i=1}^{N} \frac{P_i \sigma_{r_i,d}^2 - P_s \sigma_{s,r_i}^2 e^{B_{c_i}} \left(\mathcal{E} + \ln B_{c_i}\right)}{P_i} \right\}, \text{ subject to } P_s + \sum_{i=1}^{N} P_i \leq P, \quad P_i \geq 0 \quad \forall i. \quad (52)$$

TABLE I
DiffAF: OPTIMUM POWER ALLOCATION FOR COOPERATION SYSTEM WITH ONE RELAY BASED ON EXHAUSTIVE SEARCH AND APPROXIMATE CLOSED-FORM FORMULATION (55)

$[\sigma^2_{s,d}, \sigma^2_{s,r_i}, \sigma^2_{r_i,d}]$	DBPSK $[a_s, a_1]$		DQPSK $[a_s, a_1]$	
	Exhaustive	Approximate	Exhaustive	Approximate
$[1,1,1]$	[0.66, 0.34]	[0.66, 0.34]	[0.70, 0.30]	[0.69, 0.31]
$[1,10,1]$	[0.54, 0.46]	[0.54, 0.46]	[0.54, 0.46]	[0.54, 0.46]
$[1,1,10]$	[0.80, 0.20]	[0.79, 0.21]	[0.80, 0.20]	[0.78, 0.22]

TABLE II
DiffAF: OPTIMUM POWER ALLOCATION FOR COOPERATION SYSTEM WITH TWO RELAYS BASED ON EXHAUSTIVE SEARCH AND APPROXIMATE FORMULATION (56)

$[\sigma^2_{s,d}, \sigma^2_{s,r_i}, \sigma^2_{r_i,d}]$	DBPSK $[a_s, a_1, a_2]$		DQPSK $[a_s, a_1, a_2]$	
	Exhaustive	Approximate	Exhaustive	Approximate
$[1,1,1]$	[0.46, 0.33, 0.21]	[0.49, 0.26, 0.26]	[0.48, 0.33, 0.19]	[0.50, 0.25, 0.25]
$[1,10,1]$	[0.44, 0.28, 0.28]	[0.47, 0.27, 0.27]	[0.40, 0.30, 0.30]	[0.39, 0.31, 0.30]
$[1,1,10]$	[0.65, 0.21, 0.14]	[0.65, 0.17, 0.17]	[0.66, 0.21, 0.13]	[0.67, 0.16, 0.16]

$Q(c_i, q)$ in (A-5) contains power allocation of each relay inside the summation. To reduce complexity of the search space, we remove the summation inside $Q(c_i, q)$ such that the approximate $Q(c_i, q)$ depends only on the c_i of interest. Therefore, an optimum power allocation can be approximately obtained by finding q such that

$$(N+1)q - \frac{1}{c_i} + \frac{\sigma^2_{r_i,d} + \sigma^2_{s,r_i} \Upsilon e^{B_{c_i}} \left[\frac{1}{Pq}(\mathcal{E} + \ln B_{c_i}) + \frac{1}{B_{c_i}}\right]}{c_i^2[c_i\sigma^2_{r_i,d} - \sigma^2_{s,r_i} e^{B_{c_i}}(\mathcal{E} + \ln B_{c_i})]} - \frac{1}{P}\frac{\sigma^2_{s,r_i}\Upsilon e^{B_{c_i}}\left(\mathcal{E} + \ln B_{c_i} + \frac{1}{B_{c_i}}\right)}{c_i[c_i\sigma^2_{r_i,d} - \sigma^2_{s,r_i} e^{B_{c_i}}(\mathcal{E} + \ln B_{c_i})]} = 0$$

and

$$1 + \sum_{i=1}^{N} c_i(q) - \frac{1}{q} = 0 \qquad \forall i, i = 1, \ldots, N. \tag{56}$$

From (56), the optimum power allocation that involves $(N+1)$-dimensional search is reduced to single-dimensional search over the parameter q, $q \in (0,1)$. Table II summarizes the numerical search results from the multidimensional search based on (49) in comparison with those from approximate one-dimensional search using (56). Based on the optimization problem (56), the searching time for optimum power allocation can be greatly reduced, while the obtained power allocation is very close to that from solving (49) using multidimensional search.

From the results in Tables I and II, we can also observe that, for any channel link qualities, more power should be allocated at the source so as to maintain link reliability. This observation holds true for both DBPSK and DQPSK modulations. When the channel link qualities between the source and the relays are good (e.g., $[\sigma^2_{s,d}, \sigma^2_{s,r_i}, \sigma^2_{r_i,d}] = [1, 10, 1,]$), the system replicates the multiple transmit antenna system. Therefore, almost equal powers should be allocated at the source and all the relays.

B. Optimizing Power Allocation and Thresholds for the DiffDF Scheme

In this section, we determine the performance improvement of the DiffDf scheme through the joint optimization of power allocation and thresholds based on the BER lower bound (46). Specifically, for a fixed total power $P = P_s + \sum_{i=1}^{N} P_i$, we jointly optimize the threshold ζ_i, the power allocation at the source $a_s = P_s/P$, and the power allocation at each of the ith relay $a_i = P_i/P$ with an objective to minimize the BER lower bound (46)

$$(\{\hat{\zeta}_i\}_{i=1}^N, \hat{a_s}, \{\hat{a_i}\}_{i=1}^N) = \arg \min_{\{\zeta_i\}_{i=1}^N, a_s, \{a_i\}_{i=1}^N} P_b^{lb,DF}(\{\zeta_i\}_{i=1}^N, a_s, \{a_i\}_{i=1}^N) \tag{57}$$

where $P_b^{lb,DF}(\{\zeta_i\}_{i=1}^N, a_s, \{a_i\}_{i=1}^N)$ results from substituting $P_s = a_s P$ and $P_i = a_i P$ into (46). However, joint optimization in (57) involves $(2N+1)$-dimensional searching, which includes $N+1$ power allocation ratios and N decision thresholds. To make the optimization problem tractable and to get some insights on the optimum power allocation and the optimum thresholds, each relay is assumed to be allocated with the same transmitted power, and the decision thresholds are assumed the same at the destination for each relay-destination link. Accordingly, the source is allocated with power $a_s = P_s/P$ and every relay is allocated with power $a_i = (1 - a_s)/N$. Hence, the search space for this optimization problem reduces to two-dimensional searching over a_s and ζ

$$(\zeta^*, a_s^*) = \arg \min_{\zeta, a_s} P_b^{lb,DF}(\zeta, a_s, \{a_i\}_{i=1}^N) \tag{58}$$

where $P_b^{lb,DF}(\zeta, a_s, \{a_i\}_{i=1}^N)$ results from substituting $\zeta_i = \zeta$, $P_s = a_s P$, and $P_i = (1 - a_s)P/N$ into (46).

Table III summarizes the obtained power allocation and thresholds based on the optimization problem (58). The DBPSK and DQPSK cooperation systems with two relays are considered, and different channel variances are used to investigate power allocation and thresholds for different cooperation

TABLE III
DiffDF: OPTIMUM POWER ALLOCATION AND THRESHOLDS FOR A COOPERATION SYSTEM WITH TWO RELAYS

$\left[\sigma^2_{s,d}, \sigma^2_{s,r_i}, \sigma^2_{r_i,d}\right]$	DBPSK	DQPSK
	$[a_s, a_1, a_2, \zeta]$	$[a_s, a_1, a_2, \zeta]$
$[1, 1, 1]$	[0.50, 0.25, 0.25, 0.4]	[0.52, 0.24, 0.24, 0.4]
$[1, 10, 1]$	[0.44, 0.28, 0.28, 0.4]	[0.40, 0.30, 0.30, 0.4]
$[1, 1, 10]$	[0.68, 0.16, 0.16, 1.6]	[0.70, 0.15, 0.15, 1.8]

network setups. From the results in Table III, even though the obtained power allocation is suboptimum, it provides some insightful information on how much power should be allocated to improve the system performance. In particular, as the channel quality of the relay-destination links increases, the threshold should be increased and more power should be allocated at the source to maintain link reliability. For example, if all the channel links are of the same quality, about half of the transmitted power should be allocated at the source and the optimum threshold should be 0.4. On the other hand, if the channel link between each relay and the destination is very good, then the optimum power allocation at the source increases to about 70% of the transmitted power, and the optimum threshold increases to 1.6 and 1.8 for DBPSK and DQPSK modulations, respectively.

V. SIMULATION RESULTS

We simulate the DiffAF and the DiffDF schemes with DBPSK and DQPSK modulations. We consider the scenarios where two or three relays ($N = 2$ or 3) are in the networks. The channel coefficients follow the Jakes' model [24] with Doppler frequency $f_D = 75$ Hz and normalized fading parameter $f_D T_s = 0.0025$, where T_s is the sampling period. The noise variance is assumed to be one ($\mathcal{N}_0 = 1$). The average BER curves are plotted as functions of $P/\mathcal{N}_0$.

A. Simulation Results for the DiffAF Scheme

Fig. 3(a) shows the performance of the DiffAF scheme with DBPSK modulation for a network with two relays. The simulation is performed under equal channel variances, i.e., $\sigma^2_{s,d} = \sigma^2_{s,r_i} = \sigma^2_{r_i,d} = 1$, and equal power allocation strategy ($P_s = P_1 = P_2 = P/3$). We can see that the exact theoretical BER benchmark well matches the simulated BER curve. In addition, the BER upper bound, the simple BER upper bound, and the two simple BER approximations are tight to the simulated curve at high SNR. The BER curve for coherent detection is also shown in the figure; we observe a performance gap of about 4 dB between the DiffAF scheme and its coherent counterpart at a BER of 10^{-3}.

In Fig. 3(b), we illustrate BER performance of the DiffAF scheme with DQPSK modulation when using different number of relays (N). The simulation scenario is the same as that of Fig. 3(a), and we consider two possible numbers of relays, namely, $N = 2$ and $N = 3$. It is apparent that the proposed DiffAF scheme achieves higher diversity orders as N increases. Specifically, as N increases from 2 to 3, we observe about 1.7–2-dB gain at a BER of 10^{-3}. This observation confirms our theoretical analysis in Section III-A. Also in this figure,

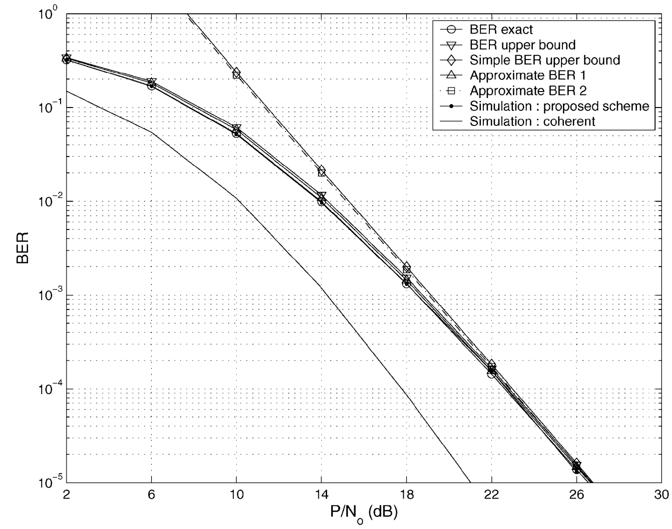

(a)

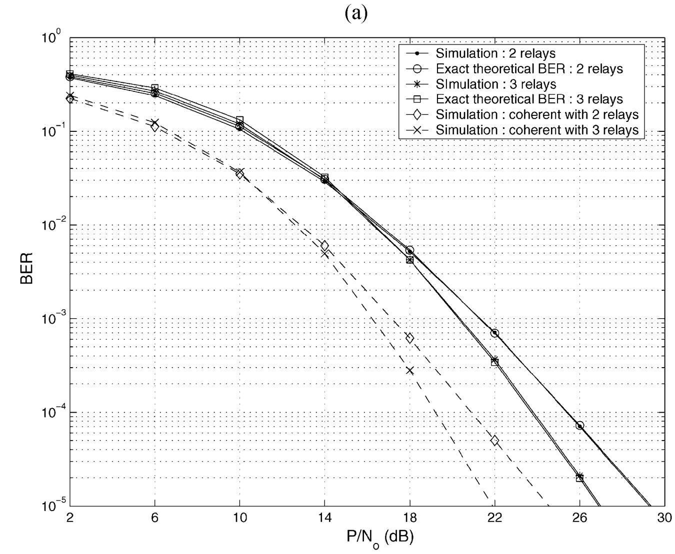

(b)

Fig. 3. DiffAF scheme with equal power allocation strategy and $\sigma^2_{s,d} = \sigma^2_{s,r_i} = \sigma^2_{r_i,d} = 1$. (a) DBPSK: two relays. (b) DQPSK: two and three relays.

the exact theoretical BER curves for $N = 2$ and $N = 3$ are tight to the corresponding simulated curves. In addition, the performance curves of the DiffAF scheme are about 4 dB away from their coherent counterparts.

Fig. 4(a) shows the BER performance of the DiffAF scheme with optimum power allocation in contrast to that with equal power allocation. We consider the DiffAF scheme with DQPSK modulation for a network with two relays. The channel variances are $\sigma^2_{s,d} = \sigma^2_{r_i,d} = 1$ and $\sigma^2_{s,r_i} = 10$, and the optimum power allocation is $[0.39, 0.31, 0.30]$ (from Table II). The simulated curves show that when all relays are close to the source, i.e., $\sigma^2_{s,r_i} = 10$, the DiffAF scheme with optimum power allocation yields about 0.6-dB gain over the scheme with equal power allocation at a BER of 10^{-3}. We observe a small performance gain in this scenario because the signal at the relays is as good as the signal at the source. Therefore, the scheme with equal power allocation yields almost as good performance as performance under optimal power allocation such that there is a small room for improvement. Also in this figure, the exact theoretical

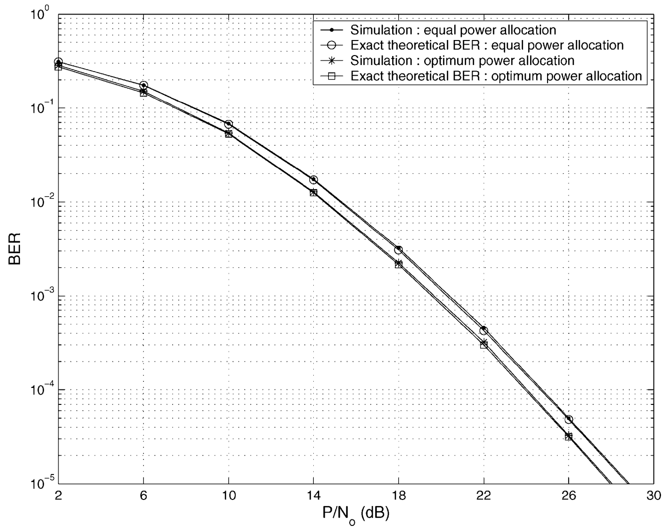

(a)

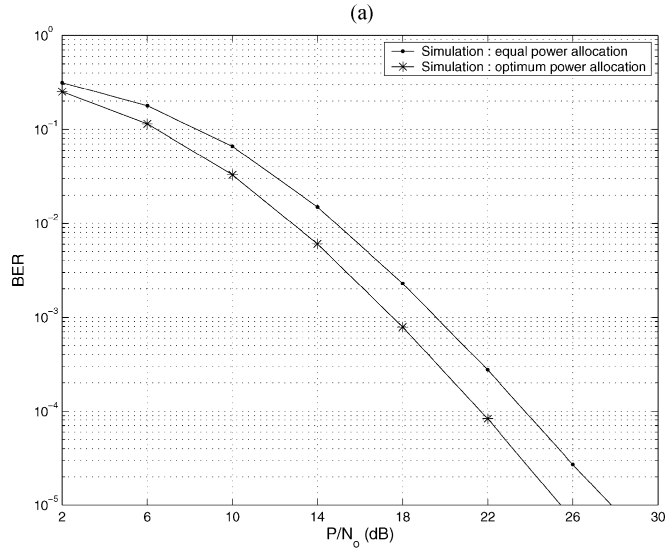

(b)

Fig. 4. DiffAF scheme with DQPSK: two relays, optimum power allocation strategy. (a) $\sigma^2_{s,d} = 1$, $\sigma^2_{s,r_i} = 10$, and $\sigma^2_{r_i,d} = 1$. (b) $\sigma^2_{s,d} = \sigma^2_{s,r_i} = 1$ and $\sigma^2_{r_i,d} = 10$.

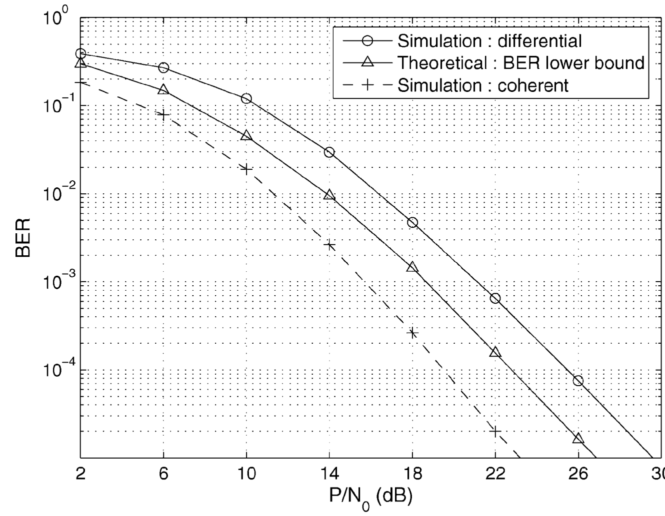

(a)

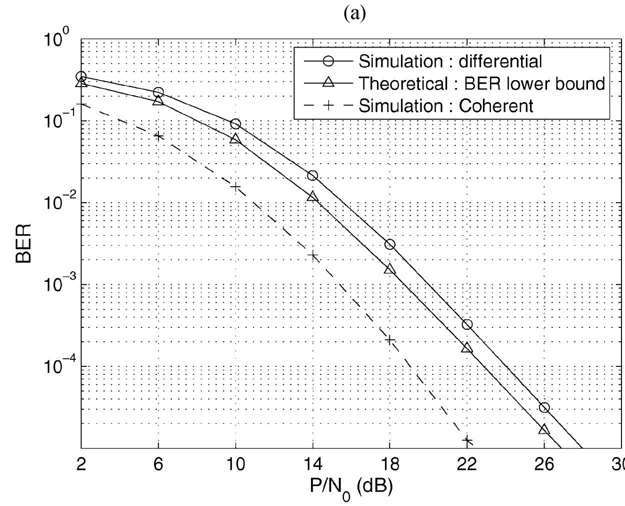

(b)

Fig. 5. DiffDF scheme with DQPSK: $\sigma^2_{s,d} = \sigma^2_{s,r_i} = \sigma^2_{r_i,d} = 1$, and $\zeta = 1$. (a) Equal power allocation. (b) Optimum power allocation.

BER curves are provided for both power allocation schemes, and they closely match their corresponding simulated curves.

In Fig. 4(b), we consider the BER performance of optimum power allocation scheme for a DQPSK cooperation system with two relays. The channel variances are $\sigma^2_{s,d} = \sigma^2_{s,r_i} = 1$ and $\sigma^2_{r_i,d} = 10$, which corresponds to a scenario that all relays are close to the destination. The optimum power allocation for this scenario is $[0.67, 0.16, 0.16]$ (from Table II). We observe that the performance with optimum power allocation is about 2 dB superior to that with equal power allocation at a BER of 10^{-3}. In this scenario, we observe a larger performance gain than the case of $\sigma^2_{s,d} = \sigma^2_{r_i,d} = 1$ and $\sigma^2_{s,r_i} = 10$ in Fig. 4(a). The reason is that using equal power allocation in this case leads to low quality of the received signals at the relays, and thus causes higher chance of decoding error at the destination based on the combined signal from the cooperative links. With optimum power allocation, more power is allocated at the source, and consequently, the quality of the received signals at the relays is improved. This results in more reliable combined signal at the destination, hence yielding better system performance.

B. Simulation Results for the DiffDF Scheme

Fig. 5(a) compares the BER lower bound with the simulated performance. We consider a DQPSK cooperation system with two relays. All nodes are allocated with equal power. The decision threshold is set at $\zeta = 1$ and the channel variances are $\sigma^2_{s,d} = \sigma^2_{s,r_i} = \sigma^2_{r_i,d} = 1$ for all i. We can see from this figure that the BER lower bound yields the same diversity order as that from the simulated performance even though there is a 2-dB performance gap between these two curves. Also in this figure, the performance of the DiffDF scheme is 5 dB away from the performance with coherent detection at a BER of 10^{-3}. An interesting observation is that when the transmitted powers are optimally allocated ($P_s = 0.6P$ and $P_i = 0.2P$) at a fixed threshold of $\zeta = 1$, as shown in Fig. 5(b), the performance gap between the simulated performance and the BER lower bound is reduced to about 1 dB at a BER of 10^{-3}. It is worth noting

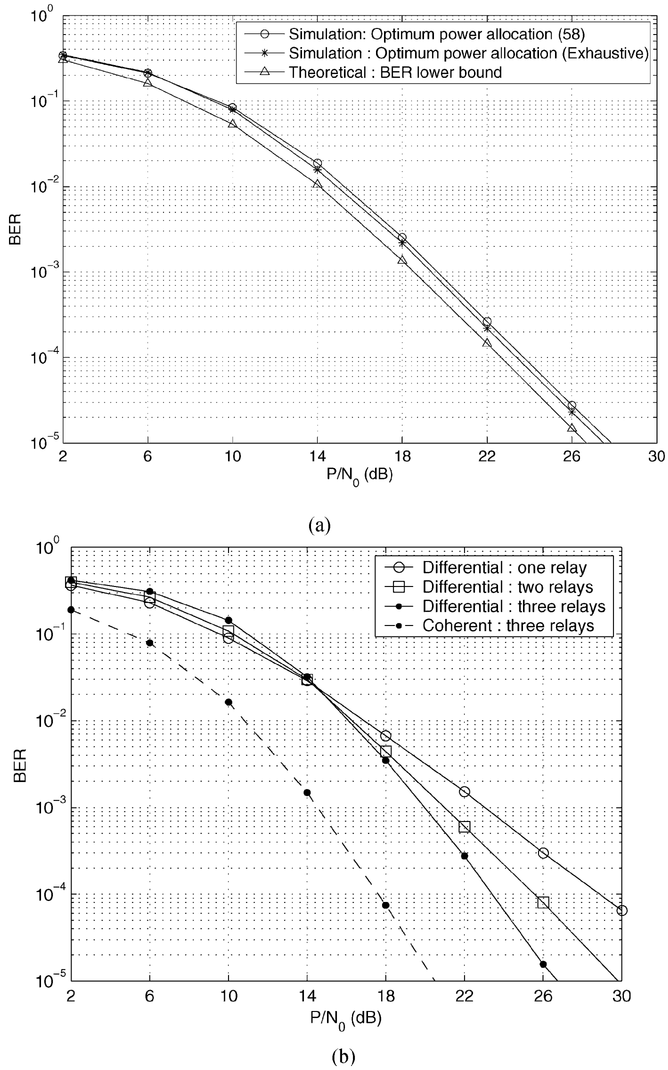

Fig. 6. DiffDF with DQPSK. (a) Optimum power allocation (58) and exhaustive optimum power allocation $\sigma^2_{s,d} = \sigma^2_{s,r_1} = \sigma^2_{r_i,d} = 1$ and $\sigma^2_{s,r_2} = 5$. (b) Different number of relays $\sigma^2_{s,d} = \sigma^2_{s,r_i} = \sigma^2_{r_i,d} = 1$.

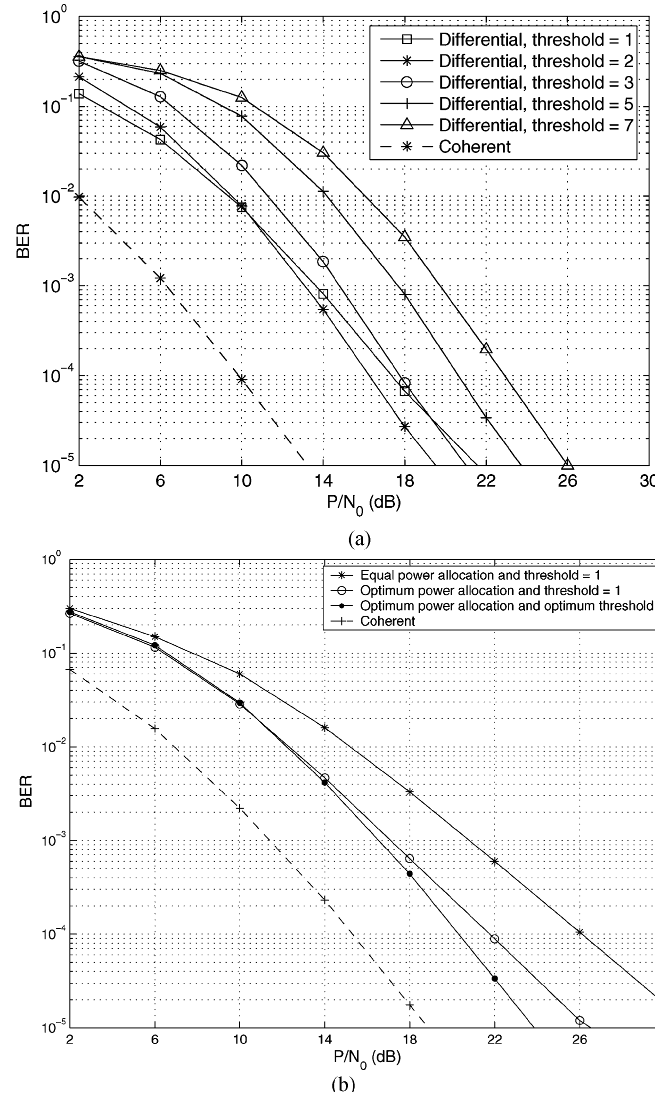

Fig. 7. DiffDF scheme with $\sigma^2_{s,d} = \sigma^2_{s,r_i} = 1, \sigma^2_{r_i,d} = 10$. (a) DBPSK: three relays, fixed power allocation, but different thresholds. (b) DQPSK: two relays, different power allocation and thresholds.

that the obtained power allocation in this scenario is the same as optimum power allocation (obtained through exhaustive numerical search). This is because the channel variances of the two relays are the same.

To receive more insight and show the merit of the optimum power allocation (58), we set up an alternative simulation scenario, which is similar to those in Fig. 5(a) and (b), but where relay 2 is located closer to the source than relay 1. We represent this scenario by setting variance of the link between the source and the relay 2 as $\sigma^2_{s,r_2} = 5$. We set the variances of all other links to one and set the threshold to one. In this case, the optimum power allocation obtained from exhaustive search is $[0.5, 0.2, 0.3]$ while the optimum power allocation obtained from (58) is $[0.6, 0.2, 0.2]$. Fig. 6(a) compares the BER performance of the two power allocation schemes. We can see from the figure that the performance with optimum power allocation (58) is almost the same as that with exhaustive optimum power allocation.

Fig. 6(b) shows the performance of the DiffDF scheme with DQPSK modulation for different number of relays. The channel variances are $\sigma^2_{s,d} = \sigma^2_{s,r_i} = \sigma^2_{r_i,d} = 1$ for all i. All nodes are allocated with equal power, and the threshold at the destination is fixed at $\zeta = 1$. We can see that the diversity order increases when higher numbers of relays are used. We observe about 3.5-dB performance improvement at a BER of 10^{-4} when the number of relays increases from one to two relays. An additional 2-dB gain at the same BER is obtained when the system increases from two to three relays. We also observe a performance gap of about 5.5 dB at a BER of 10^{-3} between the DiffDF scheme and its coherent counterpart for a cooperation system with three relays.

Fig. 7(a) shows the effect of using different thresholds on the performance of the proposed scheme. We consider a DBPSK cooperation system with three relays and all nodes allocated with equal power. The channel variances are $\sigma^2_{s,d} = \sigma^2_{s,r_i} = 1$, and $\sigma^2_{r_i,d} = 10$ for all i. Clearly, different thresholds result in different performance. Specifically, the proposed scheme with $\zeta = 2$ provides the best performance under this simulation scenario. When $\zeta = 1$, not only BER deteriorates but also the diversity order reduces. Hence, an appropriate decision threshold should be employed such that the DiffDF scheme yields reasonably good performance. Comparing the simulated performance when $\zeta = 2$ with the coherent cooperative scheme without threshold, we observe about 6-dB performance gap between the two performance curves at a BER of 10^{-3}. Such performance gap is large because in the DiffDF scheme, the CSIs are not available at the receivers, and the destination does not know whether the relay transmits or not.

In Fig. 7(b), we show the performance improvement when power allocation and decision thresholds are jointly optimized. We consider a DQPSK cooperation system with two relays. The channel variances are $\sigma_{s,d}^2 = \sigma_{s,r_i}^2 = 1$ and $\sigma_{r_i,d}^2 = 10$ for all i. In this scenario, the optimum power allocation is $a_s = 0.70$, $a_1 = 0.15$, and $a_2 = 0.15$, and the optimum threshold is $\zeta = 1.8$. We can see that the performance curve with optimum power allocation and threshold significantly improves from that with equal power allocation and an arbitrary decision threshold ($\zeta = 1$ in this case). A performance gain of 4–5 dB is observed at a BER of 10^{-3}–10^{-4}. Also in this figure, we compare the performance of optimum power allocation and threshold with that of optimum power allocation ($a_s = 0.8$, $a_1 = 0.1$, and $a_2 = 0.1$) but an arbitrary threshold ($\zeta = 1$). We can see that jointly optimizing power allocation and threshold leads to about 1–2.5-dB gain over the scheme with optimum power allocation but arbitrary threshold at BER ranges between 10^{-3} and 10^{-5}.

VI. Conclusion

In this paper, we propose differential schemes for multinode cooperative communications employing DiffAF and DiffDF cooperation protocols. In the DiffAF scheme, as a performance benchmark, we provide an exact BER expression for DMPSK modulation based on optimum combining weights. BER upper bounds and BER approximations are provided; they are tight to the simulated performance, especially at high SNR. The theoretical BER reveals that the diversity order of the proposed scheme is $N+1$ where N is the number of relays and it is confirmed by the simulation results. We observe about 1.7–2-dB gain at a BER of 10^{-3} when N increases from 2 to 3. The BER approximation is further simplified; based on the approximate BER, we are able to optimize the power allocation using a low-complexity single-dimensional search. Simulation results show that when all relays are close to the source, the proposed DiffAF scheme obtains about 0.6-dB gain over that with equal power allocation at a BER of 10^{-3}. When all relays are close to the destination, the performance with optimum power allocation achieves about 2-dB improvement over that with equal power allocation.

In case of the DiffDF scheme, we consider a multinode scenario in which each of N cooperative relays forwards only correctly decoded symbol to the destination. Decision thresholds are used at the destination to efficiently combine signal from each relay-destination link with that from direct link. An approximate BER analysis for DMPSK is provided, and a low-complexity BER lower bound is derived. The BER lower bound is very close to the simulated performance under some scenarios. While jointly optimizing power allocation and thresholds based on the BER lower bound introduces $2N+1$ dimensional searching, the search space is reduced by assuming that the same power is used at each relay and the same threshold is used at the destination. Numerical results reveal that more power should be allocated at the source and the rest should be used by the relays. In addition, larger threshold should be used when the relays are close to the destination. Simulation results show that the diversity gain of the proposed scheme increases with the number of relays. For a DBPSK cooperation system, the proposed DiffDF scheme with different thresholds leads to the performance improvement of up to 6 dB at a BER of 10^{-4}. In case of DQPSK cooperation system, the DiffDF scheme with joint optimum power allocation and optimum threshold achieves about 4–5-dB gain over that with equal power allocation and a unit threshold at a BER of 10^{-3}–10^{-4}.

Appendix
Solution to the Optimization Problem (52) by Lagrangian Method

By taking logarithm of the Lagrangian of (52) and letting $c_i = P_i/P_s$, we obtain

$$\mathcal{G} = -(N+1)\ln P_s + \lambda\left(\mathbf{c}^T\mathbf{1} - \frac{P}{P_s}\right) - \sum_{i=1}^{N}\ln c_i + \sum_{i=1}^{N}\ln\left(c_i\sigma_{r_i,d}^2 - \sigma_{s,r_i}^2 e^{B_{c_i}}\left(\mathcal{E} + \ln B_{c_i}\right)\right) \quad \text{(A-1)}$$

in which $\mathbf{c} = [1, c_1, \ldots, c_N]^T$ is an $N \times 1$ vector, and $\mathbf{1}$ denotes an $N \times 1$ vector with all ones. By differentiating (A-1) with respect to c_i and P_s and equating the results to zero, we have

$$\frac{\partial \mathcal{G}}{\partial c_i} = \lambda - \frac{1}{c_i} + \frac{\sigma_{r_i,d}^2 + \sigma_{s,r_i}^2\left[\frac{B_{c_i}e^{B_{c_i}}}{c_i}\left(\mathcal{E} + \ln B_{c_i}\right) + \frac{e^{B_{c_i}}}{c_i}\right]}{c_i\sigma_{r_i,d}^2 - \sigma_{s,r_i}^2 e^{B_{c_i}}\left(\mathcal{E} + \ln B_{c_i}\right)} = 0 \quad \text{(A-2)}$$

and

$$\frac{\partial \mathcal{G}}{\partial P_s} = -\frac{(N+1)}{P_s} + \lambda\frac{P}{P_s^2} + \sum_{i=1}^{N}\frac{\sigma_{s,r_i}^2\frac{e^{B_{c_i}}}{P_s}\left[\frac{B_{c_i}}{P_s}\left(\mathcal{E} + \ln B_{c_i}\right) + 1\right]}{c_i\sigma_{r_i,d}^2 - \sigma_{s,r_i}^2 e^{B_{c_i}}\left(\mathcal{E} + \ln B_{c_i}\right)} = 0 \quad \text{(A-3)}$$

respectively. From (A-3), we can find that

$$\lambda = (N+1)\frac{P_s}{P} - \frac{1}{P}\sum_{i=1}^{N}\frac{\sigma_{s,r_i}^2\Upsilon e^{B_{c_i}}\left(\mathcal{E} + \ln B_{c_i} + \frac{1}{B_{c_i}}\right)}{c_i\left[c_i\sigma_{r_i,d}^2 - \sigma_{s,r_i}^2 e^{B_{c_i}}\left(\mathcal{E} + \ln B_{c_i}\right)\right]} \quad \text{(A-4)}$$

in which we denote $\Upsilon \triangleq (2\mathcal{N}_0)/(b^2(1-\beta^2)\sigma_{r_i,d}^2)$. Observe from (50) that B_{c_i} can be re-expressed as $B_{c_i} = (2\mathcal{N}_0)/(b^2(1-\beta)^2\sigma_{r_i,d}^2 Pqc_i)$ where $q \triangleq P_s/P$ for $q \in (0,1)$. Then, substituting (A-4) into (A-2), we have

$$(N+1)q - \frac{1}{c_i} + \frac{\sigma_{r_i,d}^2 + \sigma_{s,r_i}^2\left[\frac{\Upsilon}{Pqc_i^2}e^{B_{c_i}}\left(\mathcal{E} + \ln B_{c_i}\right) + \frac{e^{B_{c_i}}}{c_i}\right]}{c_i\sigma_{r_i,d}^2 - \sigma_{s,r_i}^2 e^{B_{c_i}}\left(\mathcal{E} + \ln B_{c_i}\right)} - Q(c_i, q) = 0 \quad \text{(A-5)}$$

in which

$$Q(c_i, q) \triangleq \frac{1}{P}\sum_{i=1}^{N} \frac{\sigma_{s,r_i}^2 \Upsilon e^{B_{c_i}} \left(\mathcal{E} + \ln B_{c_i} + \frac{1}{B_{c_i}}\right)}{c_i\left[c_i \sigma_{r_i,d}^2 - \sigma_{s,r_i}^2 e^{B_{c_i}} \left(\mathcal{E} + \ln B_{c_i}\right)\right]}.$$

References

[1] J. N. Laneman, D. N. C. Tse, and G. W. Wornell, "Cooperative diversity in wireless networks: Efficient protocols and outage behavior," *IEEE Trans. Inf. Theory*, vol. 50, no. 12, pp. 3062–3080, Dec. 2004.

[2] A. Sendonaris, E. Erkip, and B. Aazhang, "User cooperation diversity—Part I: System description," *IEEE Trans. Commun.*, vol. 51, no. 11, pp. 1927–1938, Nov. 2003.

[3] A. Sendonaris, E. Erkip, and B. Aazhang, "User cooperation diversity—Part II: Implementation aspects and performance analysis," *IEEE Trans. Commun.*, vol. 51, no. 11, pp. 1939–1948, Nov. 2003.

[4] W. Su, A. K. Sadek, and K. J. R. Liu, "SER performance analysis and optimum power allocation for decode-and-forward cooperation protocol in wireless networks," in *Proc. IEEE Wireless Commun. Netw. Conf.*, New Orleans, LA, Mar. 2005, vol. 2, pp. 984–989.

[5] A. K. Sadek, W. Su, and K. J. R. Liu, "A class of cooperative communication protocols for multi-node wireless networks," in *Proc. IEEE Int. Workshop Signal Process. Adv. Wireless Commun.*, New York, Jun. 2005, pp. 560–564.

[6] J. N. Laneman and G. W. Wornell, "Distributed space-time coded protocols for exploiting cooperative diversity in wireless networks," *IEEE Trans. Inf. Theory*, vol. 49, no. 10, pp. 2415–2525, Oct. 2003.

[7] P. A. Anghel, G. Leus, and M. Kaveh, "Multi-user space-time coding in cooperative networks," in *Proc. IEEE Int. Conf. Acoust. Speech Signal Process.*, 2003, vol. 4, pp. 73–76.

[8] S. Barbarossa and G. Scutari, "Distributed space-time coding strategies for wideband multihop networks: Regenerative vs. nonregenerative relays," in *IEEE Proc. Int. Conf. Acoust. Speech Signal Process.*, 2004, vol. 4, pp. 501–504.

[9] M. K. Simon and M.-S. Alouini, "A unified approach to the probability of error for noncoherent and differentially coherent modulations over generalized fading channels," *IEEE Trans. Commun.*, vol. 46, no. 12, pp. 1625–1638, Dec. 1998.

[10] M. O. Hasna and M.-S. Alouini, "Performance analysis of two-hop relayed transmissions over Rayleigh fading channels," in *Proc. IEEE Veh. Technol. Conf.*, Nov. 2003, vol. 4, pp. 1992–1996.

[11] D. Chen and J. N. Laneman, "Noncoherent demodulation for cooperative diversity in wireless systems," in *Proc. IEEE Global Commun. Conf.*, Dallas, TX, Nov. 2004, pp. 31–35.

[12] P. Tarasak, H. Minn, and V. K. Bhargava, "Differential modulation for two-user cooperative diversity systems," in *Proc. IEEE Global Commun. Conf.*, Dallas, TX, Nov. 2004, pp. 3389–3393.

[13] Q. Zhao and H. Li, "Performance of differential modulation with wireless relays in Rayleigh fading channels," *IEEE Commun. Lett.*, vol. 9, no. 4, pp. 343–345, Apr. 2005.

[14] T. Himsoon, W. Su, and K. J. R. Liu, "Differential transmission for amplify-and-forward cooperative communications," *IEEE Signal Process. Lett.*, vol. 12, no. 9, pp. 597–600, Sep. 2005.

[15] T. Himsoon, W. P. Siriwongpairat, W. Su, and K. J. R. Liu, "Decode-and-forward differential modulation scheme with threshold-based decision combining," in *Proc. IEEE Wireless Commun. Netw. Conf.*, Apr. 2006, pp. 1189–1194.

[16] T. Wang, A. Cano, and G. B. Giannakis, "Link-adaptive cooperative communications without channel state information," in *Proc. IEEE Military Commun. Conf.*, Oct. 23–25, 2006, doi: 10/1109/MILCOM.2006.302370.

[17] W. P. Siriwongpairat, T. Himsoon, W. Su, and K. J. R. Liu, "Optimum threshold-selection relaying for decode-and-forward cooperation protocol," in *Proc. IEEE Wireless Commun. Netw. Conf.*, Apr. 2006, pp. 1015–1020.

[18] A. Adinoyi and H. Yanikomeroglu, "Multi-antenna aspects of wireless fixed relays," in *Proc. IEEE Wireless Commun. Netw. Conf.*, Apr. 2006, pp. 1021–1026.

[19] J. G. Proakis, *Digital Communications*, 4th ed. New York: McGraw-Hill, 2000.

[20] D. G. Brennan, "Linear diversity combining techniques," *Proc. IEEE*, vol. 91, no. 2, pp. 331–356, Feb. 2003.

[21] R. F. Pawula, "Generic error probabilities," *IEEE Trans. Commun.*, vol. 47, no. 5, pp. 697–702, May 1999.

[22] I. S. Gradshteyn, I. M. Ryzhik, and A. Jeffrey, *Table of Integrals, Series, and Products*. San Diego, CA: Academic, 1994.

[23] H. Stark and J. W. Woods, *Probability and Random Processes with Applications to Signal Processing*. Upper Saddle River, NJ: Prentice-Hall, 2001.

[24] W. C. Jakes, *Microwave Mobile Communications*. Piscataway, NJ: IEEE Press, 1993.

[25] T. Himsoon, W. P. Siriwongpairat, W. Su, and K. J. R. Liu, "Differential modulation for multi-node amplify-and-forward wireless relay networks," in *Proc. IEEE Wireless Commun. Netw. Conf.*, Apr. 2006, pp. 1195–1200.

Thanongsak Himsoon (S'03–M'07) received the B.S. degree in electrical engineering from the Chulalongkorn University, Bangkok, Thailand, in 1995 and the M.S. and Ph.D. degrees in electrical engineering from the University of Maryland, College Park, in 2001 and 2006, respectively.

Currently, he is a Communication Systems Design Engineer at Meteor Communications Corporation, Kent, WA, working on algorithm and system design for wireless communications. His research interests include signal processing, wireless communications, cooperative communications, and wireless sensor networks, with particular focus on differential modulation systems. His research contributions encompass differential space-time coding and modulation for MIMO systems, MIMO-OFDM, ultrawideband systems, and cooperative communications.

W. Pam Siriwongpairat (S'03–M'06) received the B.S. degree in electrical engineering from Chulalongkorn University, Bangkok, Thailand, in 1999 and the M.S. and Ph.D. degrees in electrical engineering from the University of Maryland, College Park, in 2001 and 2005, respectively.

Currently, she is a Wireless Communications Specialist at the Meteor Communications Corporation, Kent, WA, working on research and development of wireless communications technology. Her research interests span a broad range of areas from signal processing to wireless communications and networking, including space-time coding for multiantenna communications, cross-layer design for wireless networks, communications in mobile ad hoc networks and wireless sensor networks, OFDM systems, and ultrawideband communications.

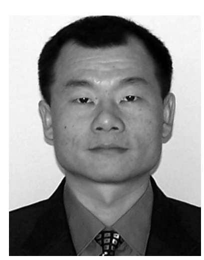

Weifeng Su (M'03) received the B.S. and Ph.D. degrees in applied mathematics from Nankai University, Tianjin, China, in 1994 and 1999, respectively, and the Ph.D. degree in electrical engineering from the University of Delaware, Newark, in 2002.

Since March 2005, he has been an Assistant Professor at the Department of Electrical Engineering, State University of New York (SUNY), Buffalo. From June 2002 to March 2005, he was a Postdoctoral Research Associate at the Department of Electrical and Computer Engineering and the Institute for Systems Research (ISR), University of Maryland, College Park. His research interests span a broad range of areas from signal processing to wireless communications and networking, including space-time coding and modulation for MIMO wireless communications, MIMO-OFDM systems, cooperative communications for wireless networks, and ultrawideband (UWB) communications.

Dr. Su received the Signal Processing and Communications Faculty Award from the University of Delaware in 2002 as an outstanding graduate student in the field of signal processing and communications. In 2005, he received the Invention of the Year Award from the University of Maryland. He has been an Associate Editor of the IEEE TRANSACTIONS ON VEHICULAR TECHNOLOGY, the IEEE SIGNAL PROCESSING LETTERS, and a Guest Editor of special issue on cooperative communications and networking of the IEEE JOURNAL OF SELECTED AREAS IN COMMUNICATIONS.

K. J. Ray Liu (F'03) is the Professor and Associate Chair, Graduate Studies and Research, and Director of Communications and Signal Processing Laboratory of Electrical and Computer Engineering Department, University of Maryland, College Park. He leads the Maryland Signals and Information Group conducting research encompassing broad aspects of information technology including signal processing, communications, networking, information forensics and security, biomedical, and bioinformatics.

Dr. Liu is the recipient of numerous honors and awards including best paper awards from the IEEE Signal Processing Society (twice), the IEEE Vehicular Technology Society, and EURASIP. He is the IEEE Signal Processing Society Distinguished Lecturer. He received the EURASIP Meritorious Service Award and National Science Foundation Young Investigator Award. He also received various teaching and research recognitions from University of Maryland including university-level Distinguished Scholar-Teacher Award, Invention of the Year Award, and college-level Poole and Kent Company Senior Faculty Teaching Award. He is Vice President—Publications. He is on the Board of Governors of IEEE Signal Processing Society. He was the Editor-in-Chief of the IEEE SIGNAL PROCESSING MAGAZINE and the founding Editor-in-Chief of *EURASIP Journal on Applied Signal Processing*.